University
of Tasmania

THERMAL AND CHEMICAL CONDITIONS OF FORMATION OF THE QUE RIVER MASSIVE SULPHIDES AND PRECIOUS METAL ZONE

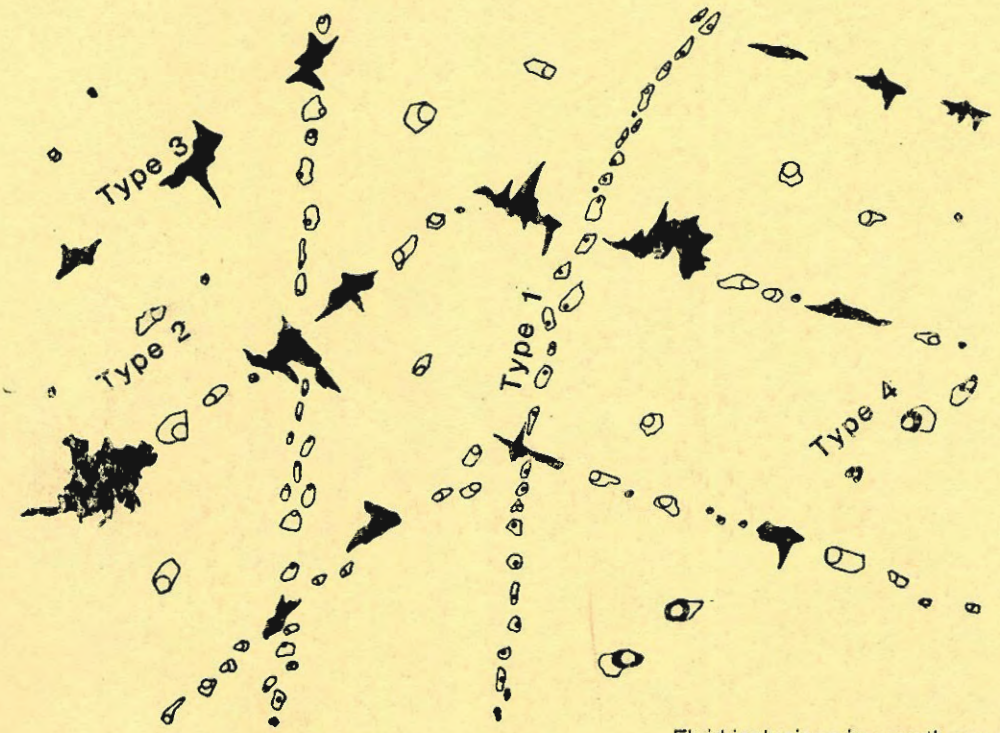

Fluid inclusions in growth zoned quartz from the Que River precious metal zone

Gregory W. Jenkins

AMIRA Report (84/P210)

April 1989

CODES Publication 20

THERMAL AND CHEMICAL CONDITIONS OF FORMATION OF THE QUE RIVER MASSIVE SULPHIDES AND PRECIOUS METAL ZONE

Gregory W. Jenkins

INTRODUCTION

The precious metal zone at Que River is an area in the northern parts of the eastern footwall containing anomalously high amounts of gold and silver relative to base metals when compared to the sulphide orebodies and the rest of the stringer system. The results of earlier work on the precious metal zone may be found in McGoldrick & Large (1987) and Jenkins (1988).

In this report, the results of fluid inclusion thermometric measurements on the precious metal zone and parts of PQ lens are presented, and further conclusions are drawn regarding the origins of the precious metal zone.

SUMMARY AND CONCLUSIONS

1. Four distinct types of fluid inclusions occur in the samples examined. Only one of these types yields information relevant to the mineralizing episode.

2. Homogenization temperatures of fluid inclusions related to the mineralizing episode span a broad range of temperatures, from 110°C to over 420°C. Only those fluids with temperatures above about 200°C are considered likely to have transported significant quantities of base metals in solution. Lower temperature fluids are considered to postdate base metal mineralization and/or to be due to mixing of hot hydrothermal fluids with seawater. However, the lower temperature fluids were capable of transporting significant quantities of gold (relative to base metals) as bisulphide complexes.

3. Most of the primary fluid inclusion contents have salinities below 5 weight percent NaCl equivalent; such fluids are considered responsible for the bulk of base metal transport. A number of fluid inclusions contain more saline fluids, and some are saturated with NaCl. The origin of the highly saline fluids is unknown at present.

4. Temperature and salinity conditions in the precious metal zone were such that the mineralizing fluids probably contained only small amounts of base metals in solution relative to gold when compared to other parts of the system, thus explaining the observed metal distribution patterns.

5. Gold transport in the precious metal zone was probably as bisulphide complexes, with precipitation due to salinity increases on mixing of hydrothermal fluids with seawater and/or decreases in sulphur fugacity due to precipitation of sulphides, particularly pyrite. There is no conclusive evidence that boiling occurred, and hence this is not considered likely to have been a mechanism for gold precipitation in this deposit. Gold precipitation in the precious metal zone may have occurred down to quite low temperatures.

6. Gold precipitation due to the change from chloride to bisulphide transport in solution probably occurred somewhere other than in the precious metal zone, perhaps within the massive sulphide orebodies. The possibility that gold precipitation occurred deeper within the stringer system must also be considered.

OCCURRENCE OF GOLD IN THE PRECIOUS METAL ZONE

The only gold observed in the precious metal zone in this study is associated with sulphides occurring in stringers up to 20cm wide or as narrow zones of massive ore which were probably separated from the main orebody during Devonian deformation. In drill core, gold values appear to correlate with stringer density.

In most samples, gold occurs with galena, either in fractures in recrystallized pyrite or in the interstices between grains of sphalerite displaying varying degrees of recrystallization. In one sample, it is also in contact with chalcopyrite.

Figures 1 to 3 show the observed occurrences of gold.

FLUID INCLUSIONS

Four different types of fluid inclusions were observed in the samples studied. The characteristics of the fluid inclusions are summarized in Table 1, and discussed below.

Type 1. These abundant fluid inclusions can be found in all samples which have not been completely recrystallized, and occasionally in strained and recrystallized quartz grains. They are interpreted as having been produced by microfracturing and subsequent healing of the fractures during Devonian metamorphism.Their metamorphic origin is confirmed by their presence in healed fractures on cleavage planes in amber sphalerite which was recrystallized during the metamorphic episode. The homogenization temperatures of all fluid inclusions of Type 1, when corrected for pressure, give trapping temperatures in the range expected for fluid inclusions produced during metamorphism to prehnite-pumpellyite grade (Jenkins 1988). No information relevant to the hydrothermal mineralization can be derived from Type 1 fluid inclusions.

Type 2. Fluid inclusions of Type 2 are relatively rare, and are only found in mineral grains which appear completely unstrained and unrecrystallized. They are similar in shape to Type 1 fluid inclusions, but they are distinct in terms of their solitary or growth plane occurrence. Their variable (in different samples) liquid:vapour ratio reflects variations in fluid characteristics in different parts of the hydrothermal system. Phase ratios within any particular generation of a mineral in the one sample are constant, implying that necking down of fluid inclusions has not occurred. Type 2 fluid inclusions provide information on the compositions and temperatures of fluids in the hydrothermal system.

Type 3. The occurrence of these vapour-rich fluid inclusions on growth surfaces of unrecrystallized quartz confirms their primary origin. Because of the very irregular shape of the fluid inclusions, any small amounts of liquid which may be present are not visible. These fluid inclusions are of distinctly different shape from Type 2 fluid inclusions, which can occur in the same grains and on the same growth surfaces as Type 3 fluid inclusions. Type 2 fluid inclusions on growth planes are usually elongate parallel to the growth planes and do not extend more than a few microns beyond the planes, while Type 3 fluid inclusions are elongate both parallel and almost perpendicular to the growth planes, and can extend for several microns or tens of microns beyond the growth planes on which they are centred. When a complete grain is viewed, the fluid inclusions sometimes appear to have a radial orientation about the C axis. The reasons for the occurrence of apparently contemporaneous Type 2 and Type 3 fluid inclusions are not clear. The very irregular shape of Type 3 fluid inclusions relative to Type 2 makes it extremely unlikely that the two types formed by necking down of larger fluid inclusions. As it is not possible to see liquid in Type 3 fluid inclusions, it is impossible to test whether they were formed by boiling, with Type 2 fluid inclusions representing the liquid phase of the boiling fluid and Type 3 representing the vapour phase. However, the difference in shape of the two fluid inclusion types argues against this possibility.

Type 4. Trails of CO_2-rich fluid inclusions of Type 4 crosscut growth planes and grain boundaries of quartz grains, and are therefore of secondary origin. Their irregular shape is similar to that of Type 3 fluid inclusions, but their occurrence in healed, sometimes curving, fractures distinguishes them.

RESULTS OF THERMOMETRIC MEASUREMENTS

Due to the scarcity of Type 2 fluid inclusions, only 16 of the 60 samples examined yielded usable thermometric data. Delays in thin section preparation made it impossible to examine more than this number of samples in the time available.

Measurements were made on stringer quartz and barite from the precious metal zone, the stringer zone below the precious metal zone, the massive ore zone (PQ lens), and and the stringer zone below the massive ore. Figure 4 shows sample locations.

Homogenization temperatures

Fluid inclusion homogenization temperatures are presented as measured without any correction for pressure, as discussed in Jenkins (1988). Pressure gradients through the hydrothermal system are unknown, and are disregarded.

Homogenization temperatures for all samples and both Type 1 and Type 2 fluid inclusions are presented in Figure 5, from which it is apparent that stringer minerals were precipitated from hydrothermal fluids over a wide range of temperatures, from 110°C to more than 420°C. Care was taken to measure only those fluid inclusions which did not show signs of necking down or leakage.

The fact that Both Type 1 and Type 2 fluid inclusions show homogenization temperatures concentrated about 180°C is problematical, as these

temperatures are lower than those generally regarded as necessary for significant base metal transport in a hydrothermal system. The coincidence of Type 2 homogenization temperatures with temperatures in the metamorphic range raises three possibilities.

(1) Some of these Type 2 fluid inclusions may be primary fluid inclusions of Devonian age, formed during complete recrystallization of the host mineral. However, complete metamorphic annealing of quartz does not occur until approximately 500°C, which is well above the metamorphic range encountered here. Also, the presence of growth zones and the euhedral nature of many of the quartz grains indicates that they have not been recrystallized, as these features would not be preserved under metamorphic recrystallization.

(2) Pressure in the hydrothermal system was high enough to necessitate the application of a substantial pressure correction. If the pressure was 500 bars, equivalent to approximately 5km depth of overlying seawater, homogenization temperatures of 150°C and 200°C would correct to temperatures of inclusion trapping of 170°C and 230°C respectively for a fluid of low salinity, and to 200°C and 250°C respectively for a fluid of 20% salinity. Thus, a combination of high salinity and high pressure would be needed to account for the observed temperatures if the fluid inclusions were trapped under conditions conducive to metal transport. While fluid inclusions of high salinity do occur in the system, the presence of low salinity, low temperature fluid inclusions and the probability of water depths shallower than 5km make it unlikely that pressure can account for the low homogenization temperatures in this system.

(3) The minerals, predominantly quartz, which host the lower temperature fluid inclusions were precipitated from cooler fluids which were not carrying appreciable quantities of base metals. This is considered the most likely explanation for the low homogenization temperatures. The cooler fluids may have been the result of general cooling of the system in its later stages, or of local mixing of hot hydrothermal fluids with cool circulating seawater causing metal precipitation elsewhere in the system, after which the metal-depleted fluids precipitated quartz and barite at the points sampled.

Figures 6,7 and 8 show homogenization temperatures in the principal areas of the system under consideration, in the different lithologies of these areas, and in the stringers and disseminated patches of different sulphide mineralogies. The high temperatures observed in the massive ore zone (BMS) are in a quartz+pyrite stringer, but are not necessarily representative. The lack of suitable samples in the BMS ore zones, which are strongly deformed and recrystallized, makes it impossible to present sufficient data on these zones to draw valid conclusions. Homogenization temperatures in the quartz+pyrite±base metal sulphide stringers below the massive ore (BMS STR) are comparable with those from the stringers below the precious metal zone (PMZ STR), while homogenization temperatures in the precious metal zone itself (PMZ) show a wider range, with measured values up to 360°C. In addition, the precious metal zone, its underlying stringers, and the massive ore contain small (~3μm) fluid inclusions with homogenization temperatures well above 420°C; decrepitation of larger fluid inclusions causing sample fracturing precluded exact measurement of homogenization temperatures of these small fluid inclusions. Most of the small, high temperature fluid inclusions were observed in the precious metal zone. It is considered unlikely that the high temperatures are the result of leakage of fluid inclusion contents.

Figure 7 shows homogenization temperatures in terms of the individual lithologies which host the stringers. The lithological names are those of the original mine classification scheme, and are used here in a purely descriptive, non-genetic sense. Highest measured temperatures occur in the LTP ("lapilli tuff") unit; these are in the samples from the massive ore zone. The widest range of temperatures occurs in the RwP ("reworked pyroclastics") unit. Temperatures in the HAT ("intensely altered volcaniclastic rock") unit are in the lower ranges.

Figure 8 shows homogenization temperatures for the main sulphide associations adjacent to and in the same stringers and disseminated patches as the transparent minerals hosting the measured fluid inclusions. The widest spread of homogenization temperatures is shown by the pyrite+sphalerite+galena (py,sp,ga) stringers and areas. This is the most common sulphide assemblage. Pyrite only (py) areas have homogenization temperatures in the lower ranges as well as a few above 420°C. Pyrite+sphalerite+galena+ chalcopyrite (py,sp,ga,cp) areas show homogenization temperatures up to 370°C and several above 420°C. Pyrite+sphalerite+ galena+tetrahedrite samples show low homogenization temperatures (<180°C) only.

Many homogenization temperatures which, when corrected for pressure, fall within the metamorphic range (homogenization temperatures 150°-200°C) were observed in fluid inclusions of Type 2. While it is possible that some of these are isolated Type 1 fluid inclusions, it is unlikely, as great care was taken to distinguish the two types before measuring.

Salinities of fluid inclusion contents

The results of measurements of the final melting temperatures of ice in fluid inclusions are presented in Figures 9,10 and 11 as weight percentage NaCl equivalent, calculated using the method of Potter *et al.* (1978). Salinities of fluid inclusions saturated with NaCl are given as 23.2% NaCl, which represents saturation at ambient temperature.

Fluid inclusions from the precious metal zone show three ranges of salinity, that is, approximately 0–5%, 7–9% and 22–23.2% (saturated, often containing halite daughter crystals). The stringer zones contain fluid inclusions with similar salinities. The plots of salinity against lithology (Fig. 10) show that the distribution of salinities is similar in all units except for RwP, in which Type 2 fluid inclusions contain only low salinity fluids. The plots of salinity against area show a predominance of low salinity fluids in the precious metal zone. Only low salinity fluids occur in the pyrite+sphalerite+galena stringers (Fig. 11), while variable salinity fluids occur in the pyrite only and pyrite+sphalerite+galena+tetrahedrite stringers. The saturated fluids in pyrite+sphalerite+galena+chalcopyrite stringers are from 2 samples only and are thus not necessarily representative.

DISCUSSION

The high temperatures of homogenization observed in the massive ore zone are consistent with the higher temperatures expected towards the centre of the hydrothermal system, and reflect one of the hottest phases of the mineralizing episode. As previously stated, the results for this zone are not necessarily representative due to the lack of suitable samples.

The broad spread of homogenization temperatures in the RwP unit implies fluid flow through this unit during most stages of the hydrothermal activity. This is to be expected due to the higher permeability of the unit relative to the other lithologies. It is possible that many of the lower temperatures are also due to mixing of hydrothermal fluids with seawater. Sulphur isotope data imply a seawater component in the hydrothermal fluids (McGoldrick, 1988). The broad homogenization temperature range of the lower (<5%) salinity fluids is considered to be due to mixing with seawater (salinity ≈3%), as well as reflecting different stages in the history of the hydrothermal system. The saturated fluids are not considered to contain a seawater component.

The LTP unit shows a similar broad spread of homogenization temperatures, but with some temperatures above 420°C. The two samples which display the higher temperatures are from base metal bearing stringers, one near the eastern footwall/ hangingwall contact adjacent to massive sulphides (503118), and the other well away from the centre of the hydrothermal system in the eastern footwall (502689). The high temperature of the former is attributed to its proximity to the hydrothermal centre, while the latter is considered an isolated stringer in which there was no mixing with seawater. Salinity measurements were not possible in either sample.

The fact that homogenization temperatures in the stringer zone below the massive sulphides are lower than in the massive sulphides themselves and in the precious metal zone is probably due to the general lack of preservation of Type 2 fluid inclusions in this area, with only lower temperature fluid inclusions occurring in the two undeformed samples examined.

The sulphide assemblages reflect the different homogenization temperatures of fluid inclusions in the associated quartz and barite (Fig. 8). In many samples, the base metal sulphides are partly corroded, and so represent an earlier stage of the paragenesis of the system, in which processes of reworking such as those proposed by Eldridge *et al.* (1983) were operating. Pyrite+sphalerite+galena stringers show a wide range of temperatures. The higher temperature fluids are considered to have been responsible for base metal transport, while the lower temperature fluids are considered to have passed through the system after base metal transport and deposition occurred, and/or to be due to mixing with seawater. Stringers and areas with pyrite have fluids which were at either low or high temperature, the low temperatures being unsuitable for base metal transport and high temperatures being unsuitable for base metal precipitation. Pyrite+sphalerite+galena+chalcopyrite stringers have a similar homogenization temperature distribution to pyrite+sphalerite+galena stringers,but with more fluid temperatures above 420°C; these fluids may have been responsible for copper transport. The two samples of pyrite+sphalerite+galena+tetrahedrite stringers showed very low homogenization temperatures. This may be significant in view of the association of tetrahedrite with gold as reported by Whitford & Creelman (1984).

Because of the relative scarcity of salinity measurements, caution should be used in drawing conclusions. The results (Figs. 9,10,11) show two main groups, those fluid inclusions with salinities less than 5%, and those saturated with respect to NaCl. A few fluid inclusions have salinities between 5% and 23%; these may have formed by mixing of NaCl-saturated fluids with seawater. Alternatively, they may be primary fluid inclusions of Devonian age, as mentioned earlier.

The most common fluids, regarded as responsible for the bulk of base metal transport, have salinities of 0 to 5%. The origin of the saturated fluids is unknown, and any discussion would be speculative.

Figure 12 shows salinity plotted against homogenization temperature for fluid inclusions associated with different sulphide assemblages, lithologies and areas, and Figure 13 shows superimposed solubility contours for Zn as chloride complexes and Au as bisulphide complexes. The homogenization temperature distribution of fluid inclusions for which salinity was not measurable is also shown. It is apparent that only the higher temperature (>≈250°C), low salinity fluids and some of the higher temperature (>≈200°C) saturated fluids could have transported significant (>≈0.5ppm) quantities of Zn in solution. However, the lower temperature fluids could have carried Au in solution as bisulphide. It may be fortuitous only, but the distribution of salinity against temperature in Figure 13 conforms very roughly to the shape of the $Au(HS)_2$ solubility contours. Thus, it is likely that in the areas studied, and particularly the precious metal zone, the circulating fluids, which were neither hot nor saline enough to carry as much base metal in solution as the fluids near the hydrothermal centre, carried significant quantities of Au in solution as bisulphide complexes. The higher solubility of Au as bisulphide in cooler, less saline fluids implies that the gold bearing fluids could cool down while moving away from the hydrothermal centre and still retain Au in solution. The low temperatures of homogenization recorded for tetrahedrite bearing stringers and the association of tetrahedrite with gold (Whitford & Creelman, 1984) support the idea of some gold transport in relatively cool fluids. The most likely causes of precipitation of gold from bisulphide complexes are an increase of salinity due to mixing of low salinity fluids with seawater (salinity ≈3%) and/or a decrease in sulphur fugacity due to precipitation of sulphides, particularly pyrite. In either case, the high Au content of the precious metal zone relative to base metals is explained.

It is important to note that, as gold was probably in solution predominantly as bisulphide complexes in the samples studied, the change from chloride transport to bisulphide transport must have occurred elsewhere in the hydrothermal system. If the solutions were saturated with respect to gold, the change in mode of transport would have caused gold precipitation (Huston & Large, 1988). This may have been in the massive sulphide orebodies, or deeper in the stringer zone. The possibility that it occurred below the orebodies should be borne in mind for exploration purposes.

APPLICATION OF FLUID INCLUSION STUDIES TO FUTURE WORK IN THE QUE RIVER AREA

Provided that relatively unrecrystallized and undeformed samples can be obtained, the study of fluid inclusions can prove a useful adjunct to exploration programs. In a deformed area such as in and around the Que River orebodies, it is necessary to produce and examine a large number of thin sections in order to find a relatively small number of useful fluid inclusions. This problem decreases in less deformed areas, but possible metamorphic effects must be borne in mind whenever regional metamorphism has affected a mineralized area, even though the effects may not be immediately visible in individual undeformed samples.

In the Que River area, the deformation of the central part of the hydrothermal system (the main sulphide orebodies) precludes the use of fluid inclusion techniques in deriving information on this part of the system. However, measurements on stringer material well below the orebodies, if such material is relatively undeformed, may indicate temperatures within the feeder system and assist in showing the possible positions of other base metal sulphide concentrations away from the known orebodies. In addition, it may be possible using temperature data to define the position at which the change from gold chloride to gold bisulphide transport occurred, and hence the position where significant amounts of gold could be precipitated from solutions saturated with gold, if this did not take place within the sulphide orebodies.

REFERENCES

Eldridge, C.S., Barton, P.B.Jr., & Ohmoto, H. (1983) Mineral textures and their bearing on formation of the Kuroko orebodies. *Econ. Geol. Monogr.*, 5, 241-281.

Huston, D.L., & Large, R.R. (1989) A chemical model for the concentration of gold in volcanogenic massive sulphide deposits. *Ore Geology Reviews* (in press).

Jenkins, G.W. (1988) Paragenesis and fluid inclusions in the Que River footwall precious metal zone. A.M.I.R.A. Project 84/P210, *Controls on gold and silver grades in volcanogenic massive sulphide deposits*. Final report, 43-46.

McGoldrick, P.J., & Large, R.R. (1987) Final report on the footwall precious metal zone, Que River. A.M.I.R.A. Project 84/P210, *Controls on gold and silver grades in volcanogenic massive sulphide deposits*. 2nd annual report, 9-45.

McGoldrick, P.J. (1988) Sulphur isotope studies at Que River. A.M.I.R.A. Project 84/P210, *Controls on gold and silver grades in volcanogenic massive sulphide deposits*. Final report, 47-52.

Potter, R.W., Clynne, M.A., & Brown, D.L. (1978) Freezing point depressions of aqueous sodium chloride solutions. *Econ. Geol.*, 73, 284-285.

Whitford, D.J., & Creelman, R.A. (1984) Petrological and geochemical studies at Que River, Part 5. *C.S.I.R.O. Division of Mineralogy, Restricted Investigation Report* 1498R.

Figure 1. Observed occurrences of gold.
A. Gold with sphalerite (sp), galena (ga), pyrite (py), quartz (qz). Sample no. 503077. Scale bar 100μm.
B. Gold at a grain boundary in sphalerite with galena, pyrite, quartz. Sample no. 503077. Scale bar 100μm.
C. Gold with galena in sphalerite , pyrite. Sample no. 503077. Scale bar 50μm.
D. Gold with galena in sphalerite, pyrite.Sample no. 503077. Scale bar 100μm.

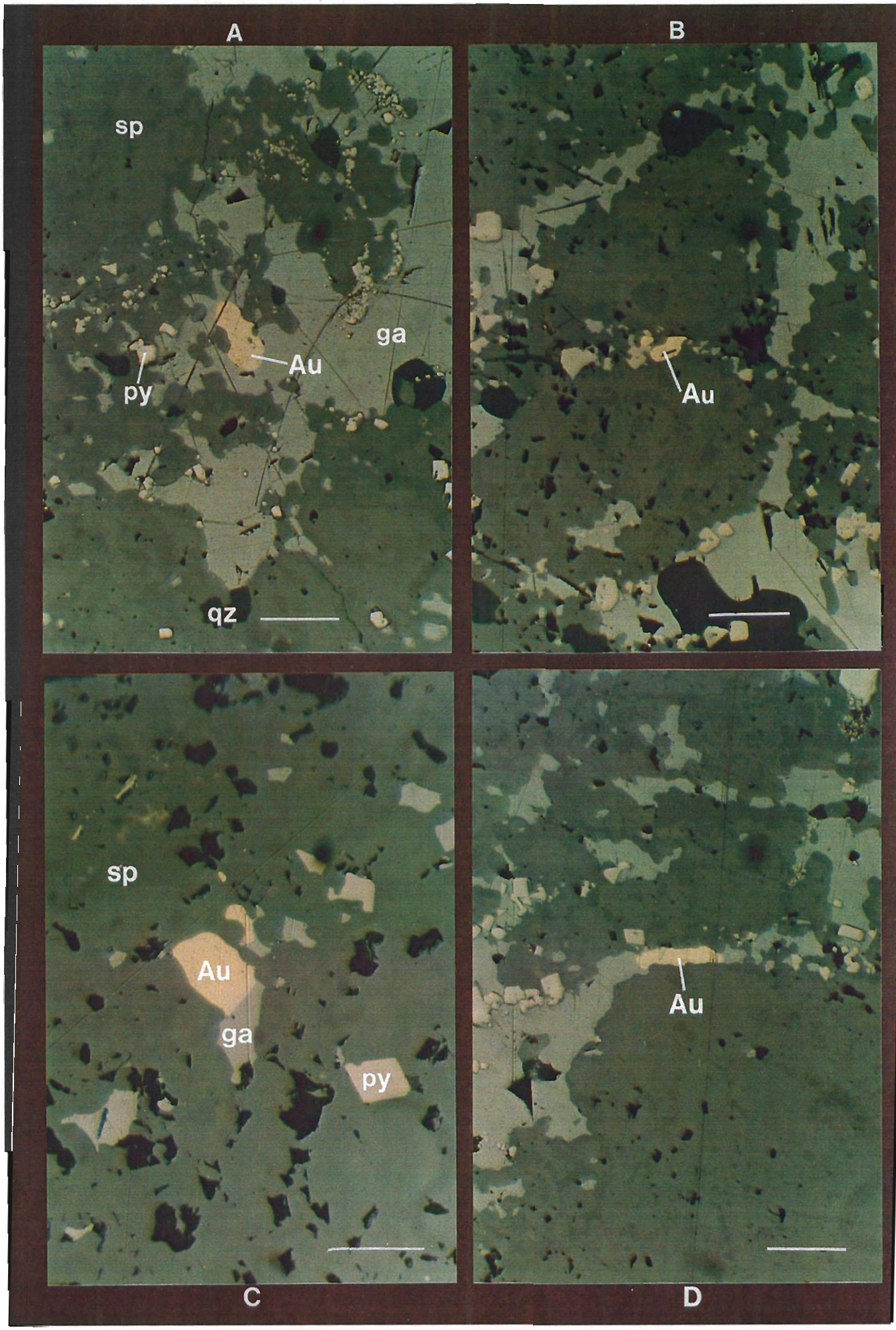
A
sp
ga
Au
py
qz
B
Au
sp
Au
ga
py
C
Au
D

Figure 2. Observed occurrences of gold.
A. Gold with galena (ga) and chalcopyrite (cp) in pyrite (py). Sample no. 503093. Scale bar 50μm.
B. Gold with galena in pyrite with sphalerite (sp), chalcopyrite, quartz (qz). Sample no. 503093. Scale bar 100μm.
C. Gold with pyrite in sphalerite. Sample no. 503003. Scale bar 50μm.
D. Gold with galena in pyrite, sphalerite. Sample no. 503080. Scale bar 50μm.

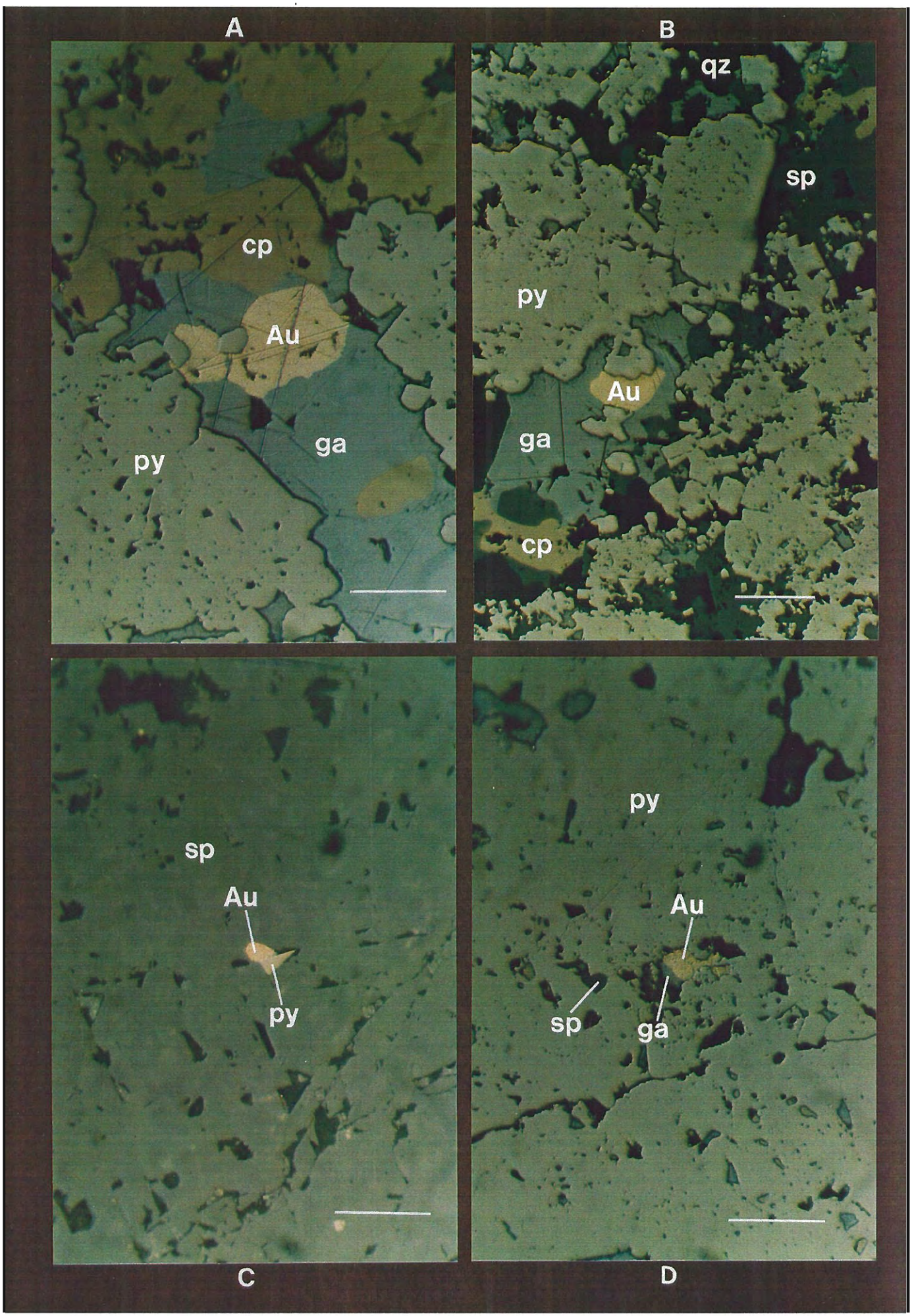
A
cp
Au
ga
py
B
qz
sp
py
Au
ga
cp
sp
Au
py
C
py
Au
sp
ga
D

Figure 3. Observed occurrences of gold.
A. Gold with galena (ga) and sphalerite (sp) in pyrite (py), quartz (qz). Sample no. 503080. Scale bar 50μm.
B. Gold with galena in pyrite. Sample no. 503080. Scale bar 50μm.
C. Gold with galena in pyrite, sphalerite, quartz, sericite (se). Sample no. 503080. Scale bar 100μm.
D. Gold with galena and sphalerite in pyrite. Sample no. 503080. Scale bar 50μm.

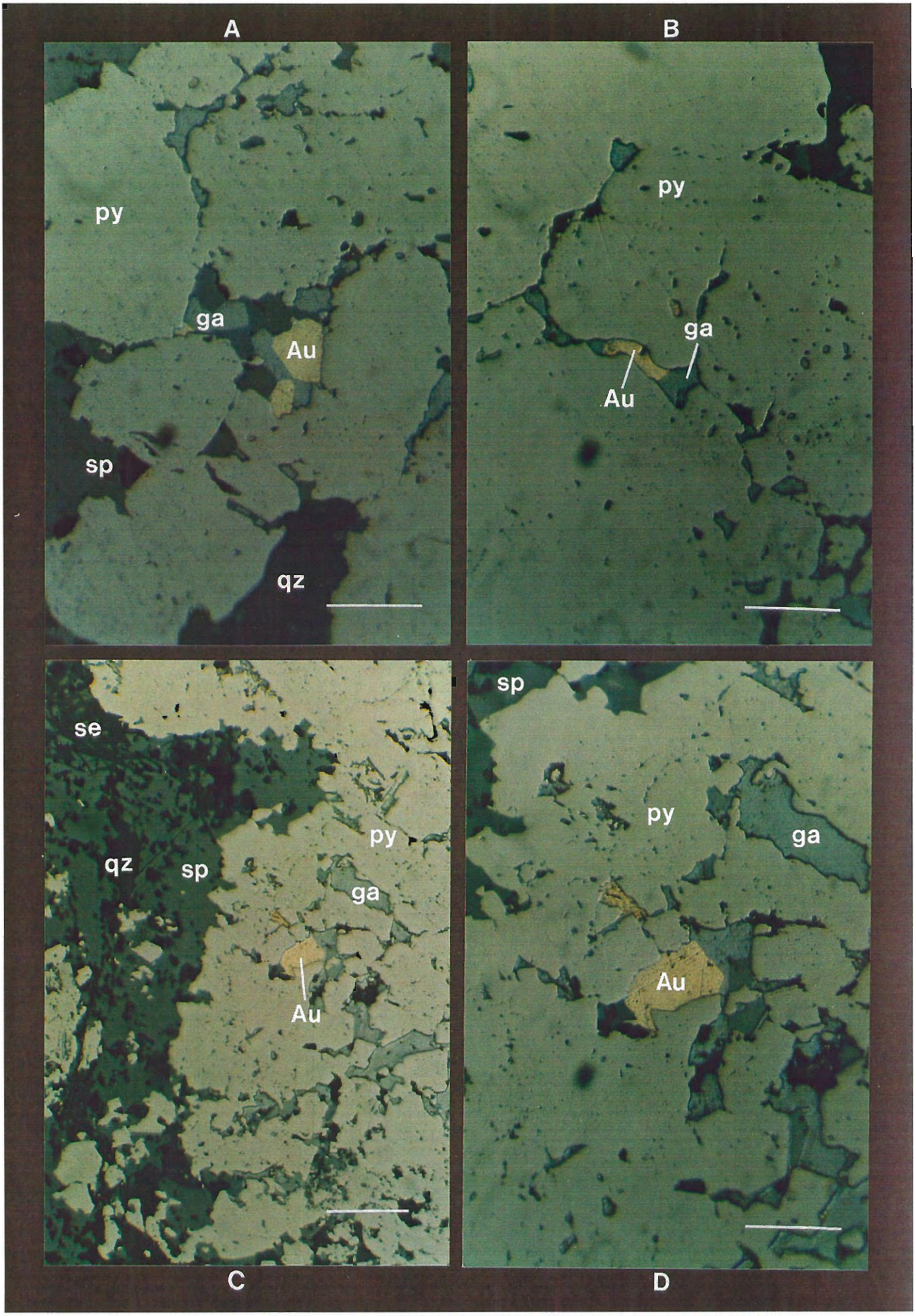
A
py
ga
Au
sp
qz
B
py
ga
Au
C
se
py
qz
sp
ga
Au
D
sp
py
ga
Au

Figure 4 (2 pages). Locations of samples used for thermometric measurement, shown on east-west cross sections through the northern parts of the Que River mineralization. Boundaries of the precious metal zone are approximate only.

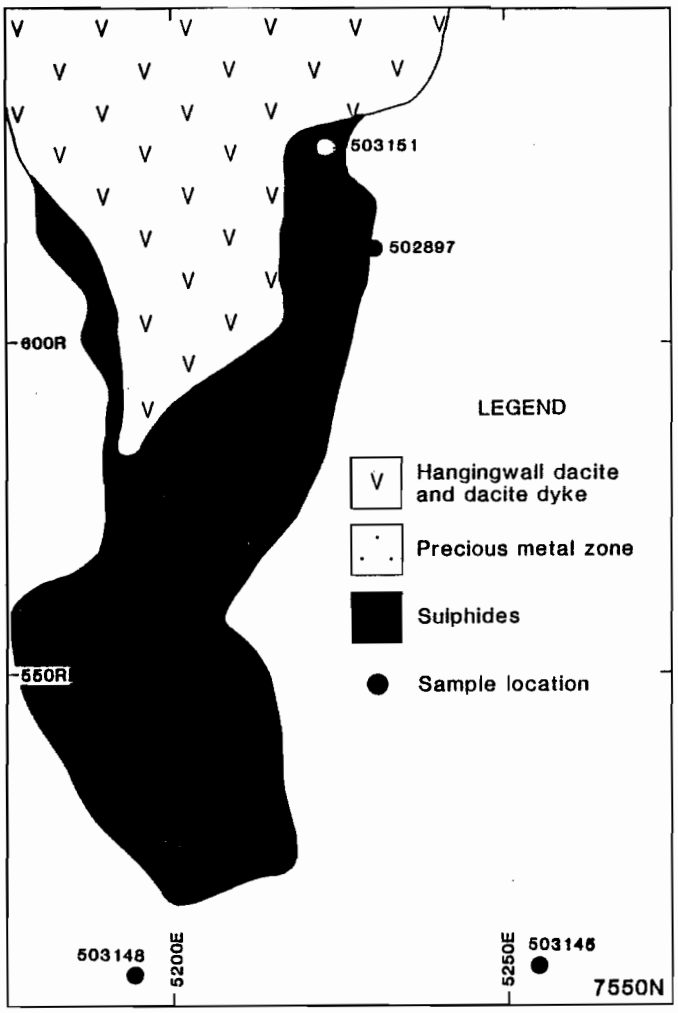
503151
502897
600R
550R
LEGEND
Hangingwall dacite and dacite dyke
Precious metal zone
Sulphides
Sample location
503148
5200E
5250E
503145
7550N

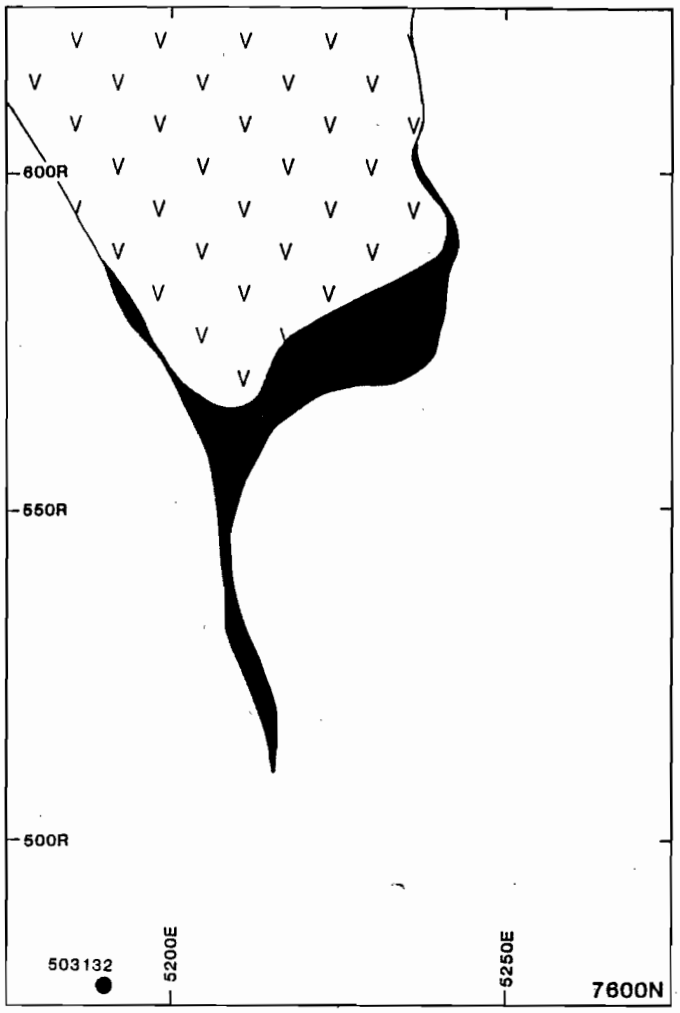
600R
550R
500R
503132
5200E
5250E
7600N

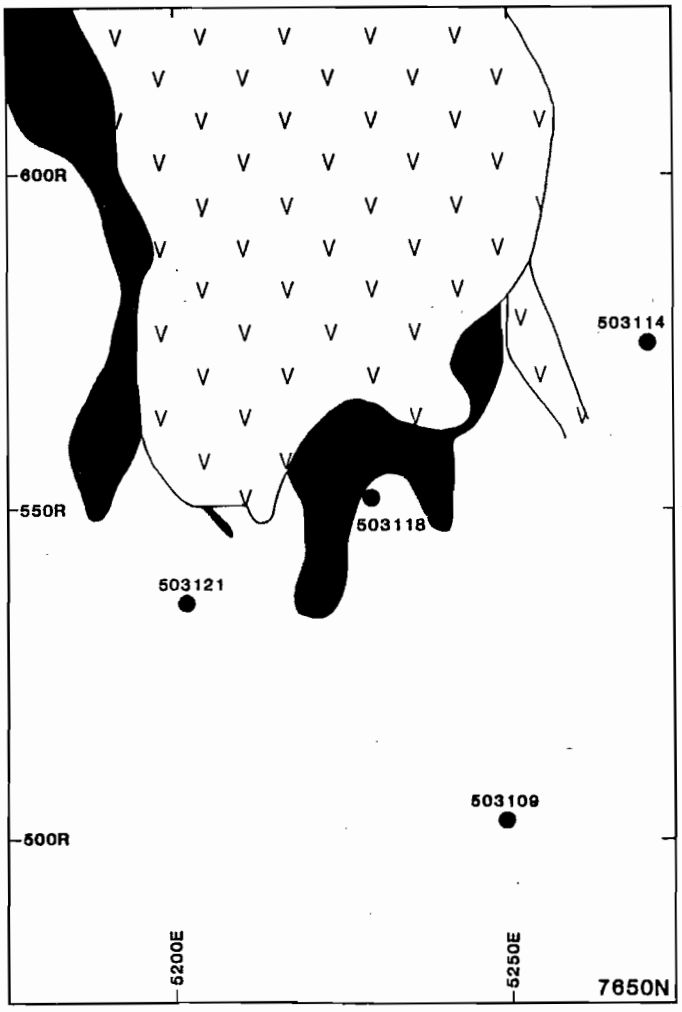
600R
550R
503114
503118
503121
503109
500R
5200E
5250E
7650N

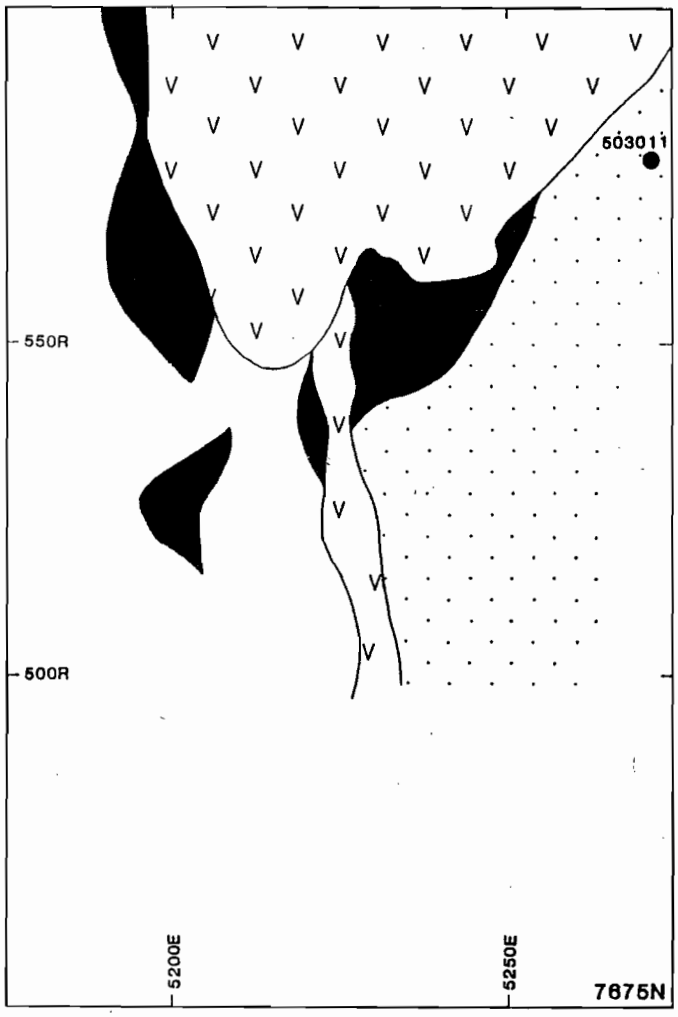
503011
550R
500R
5200E
5250E
7675N

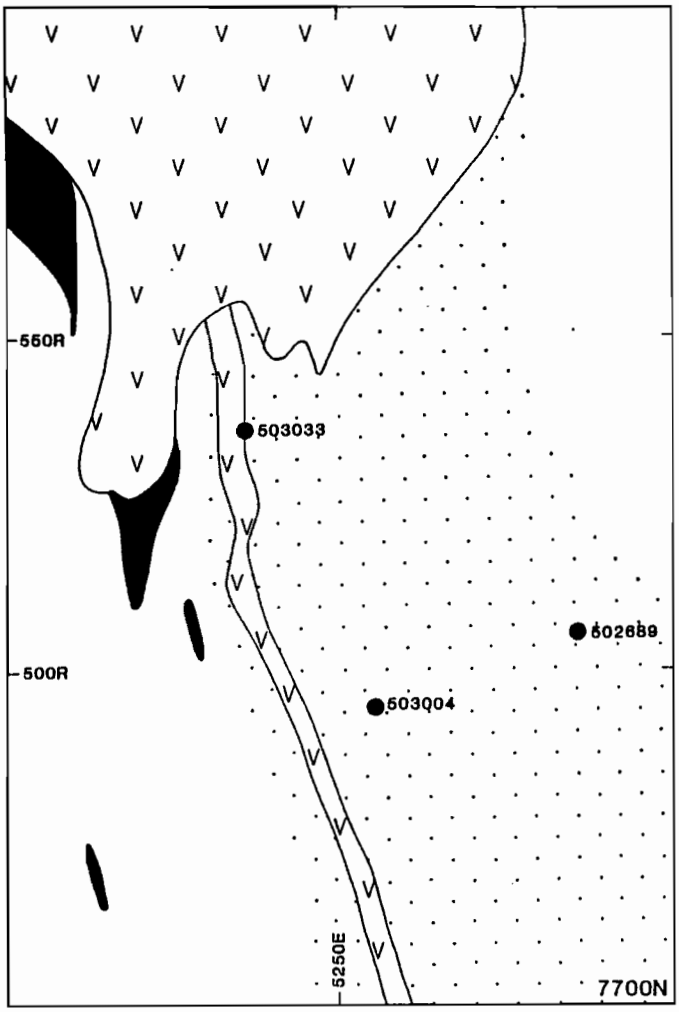
550R
503033
502689
500R
503004
5250E
7700N

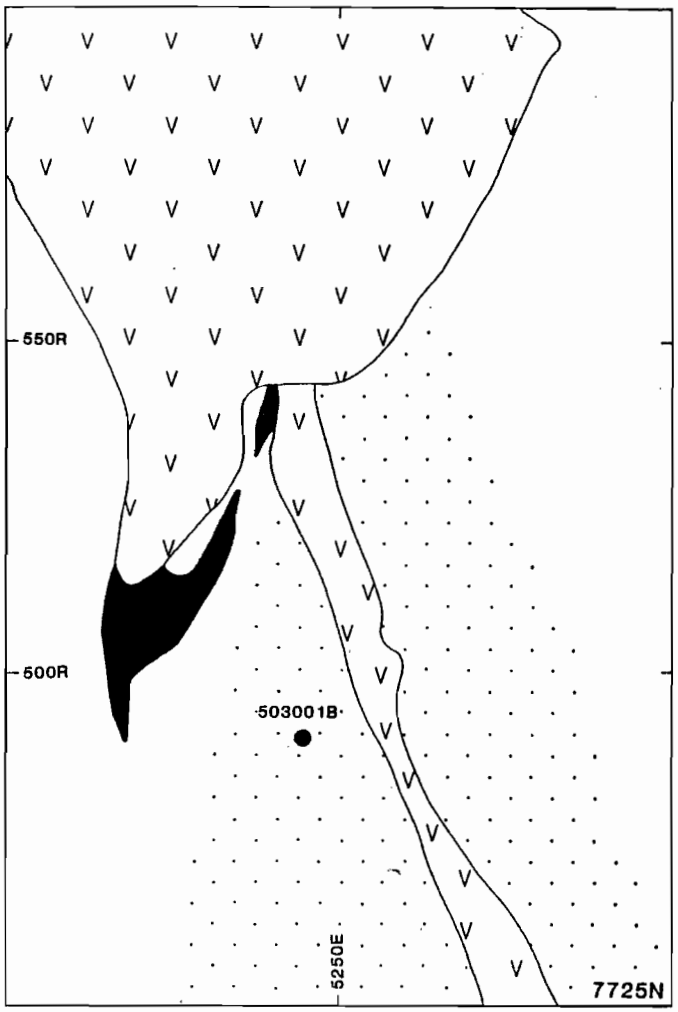
550R
500R
503001B
5250E
7725N

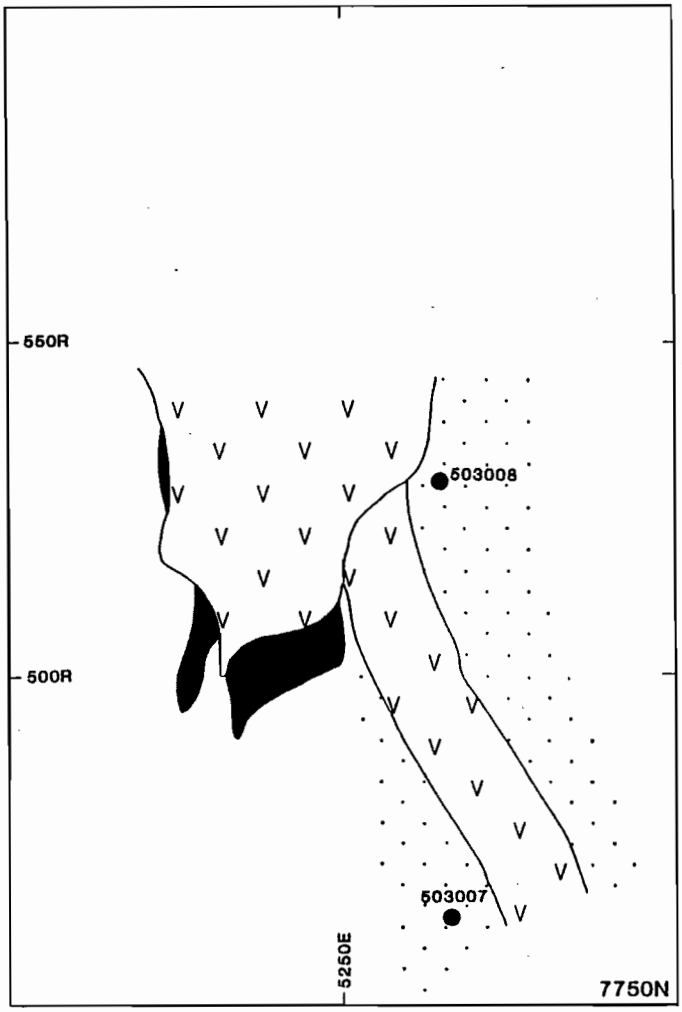
550R
503008
500R
503007
5250E
7750N

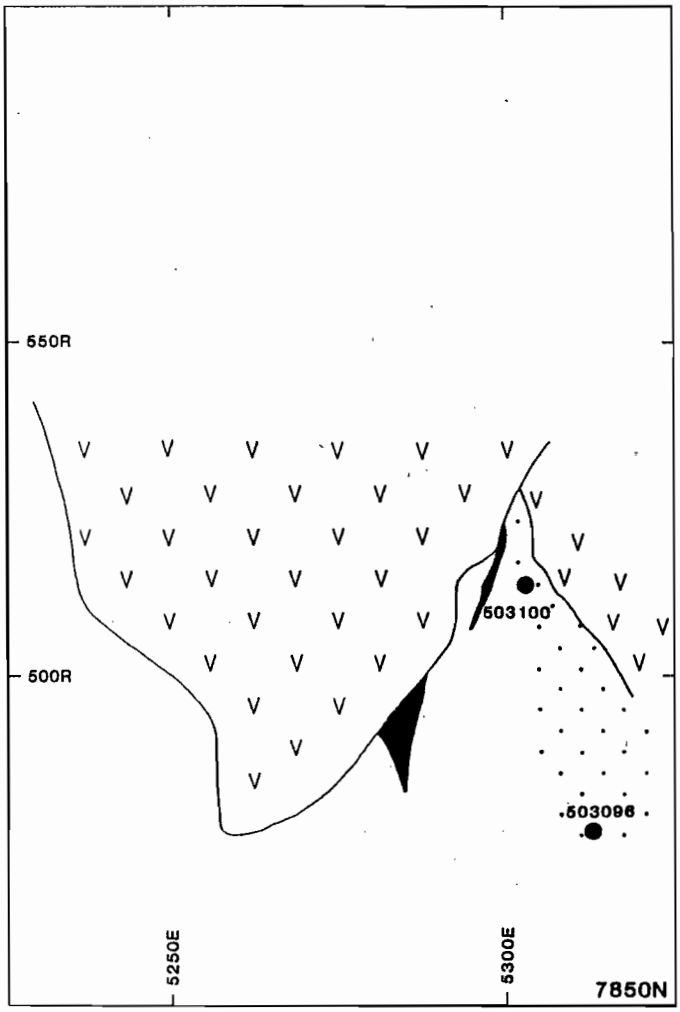
550R
503100
500R
503096
5250E
5300E
7850N

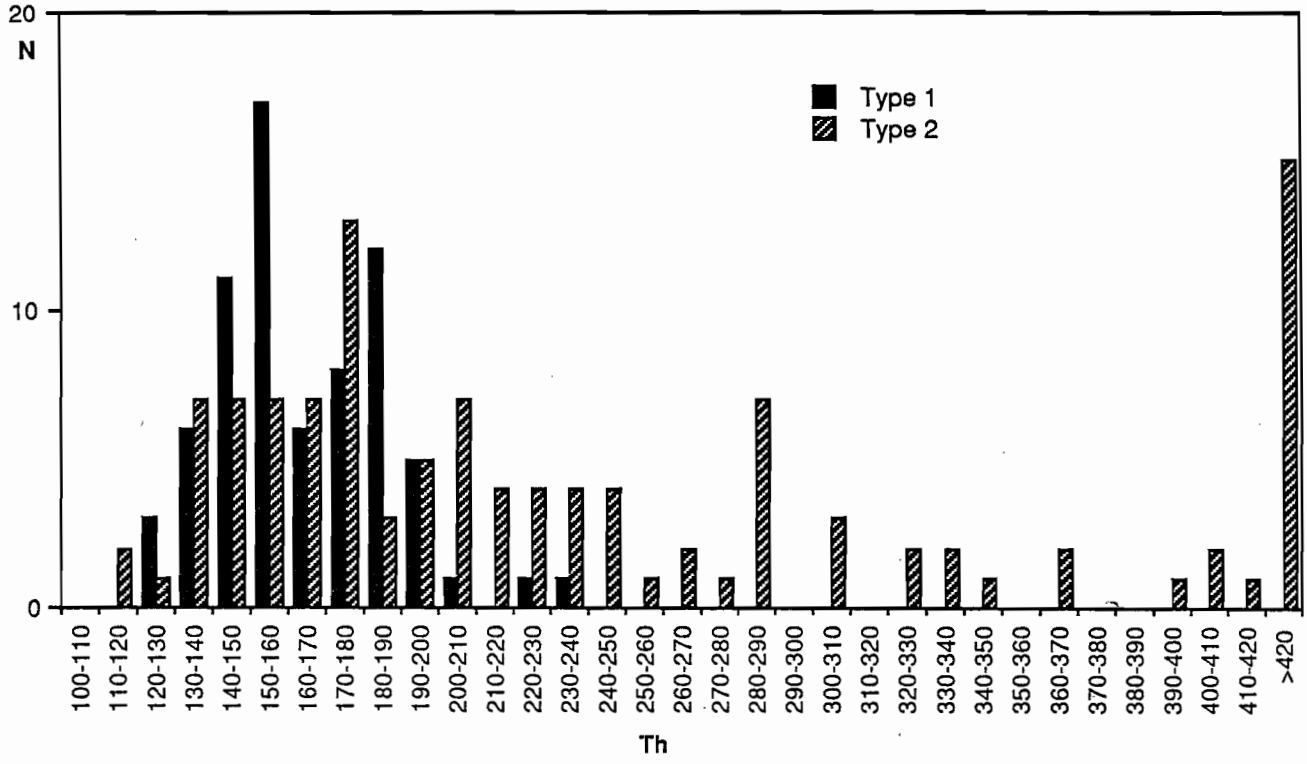

Figure 5. Homogenization temperatures of all fluid inclusions of Type 1 (secondary) and Type 2 (primary).

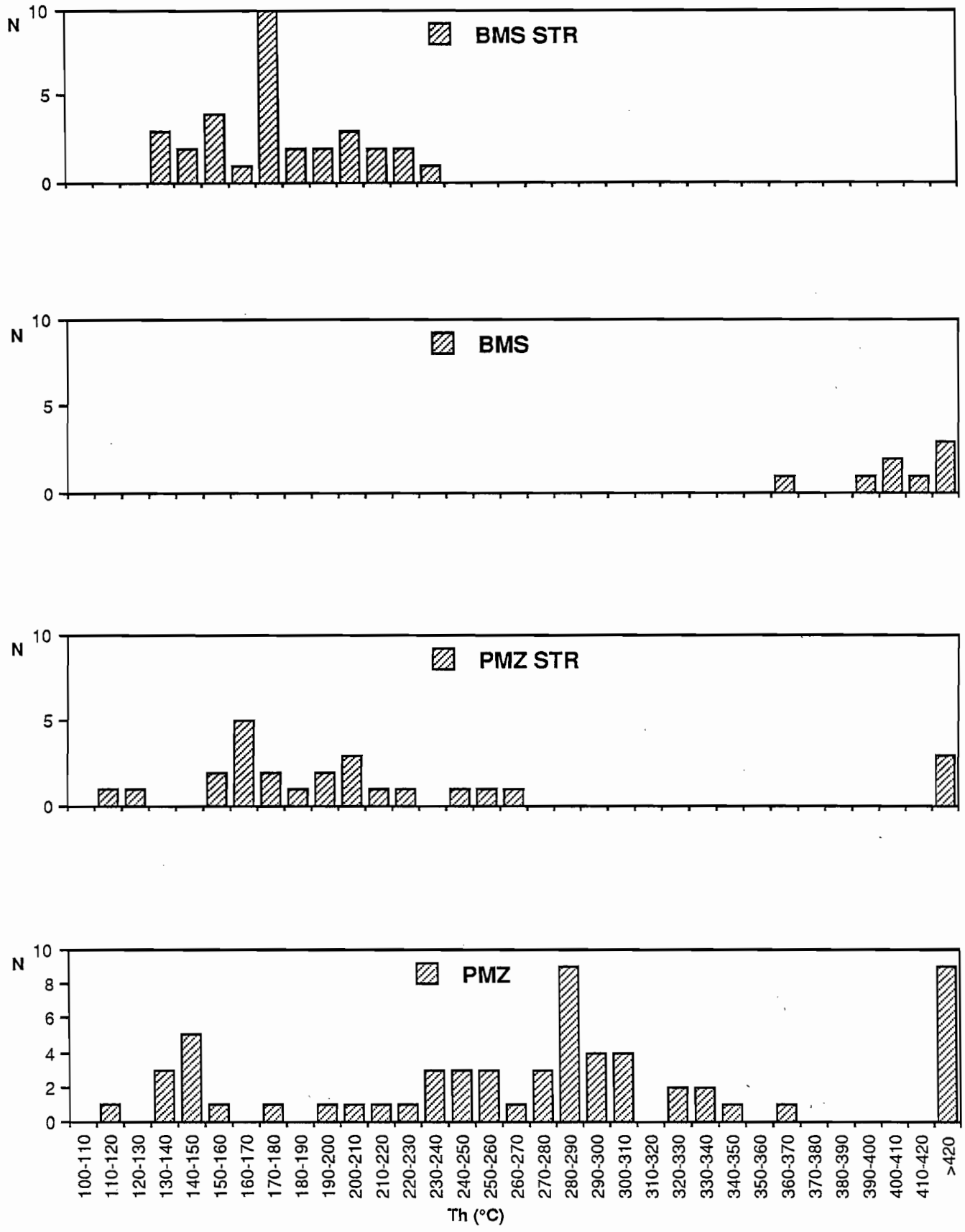

Figure 6. Homogenization temperatures of Type 2 fluid inclusions in different parts of the system. BMS STR=stringers below sulphide orebodies, BMS=base metal sulphides, PMZ STR=stringers in lower part of precious metal zone, PMZ=precious metal zone.

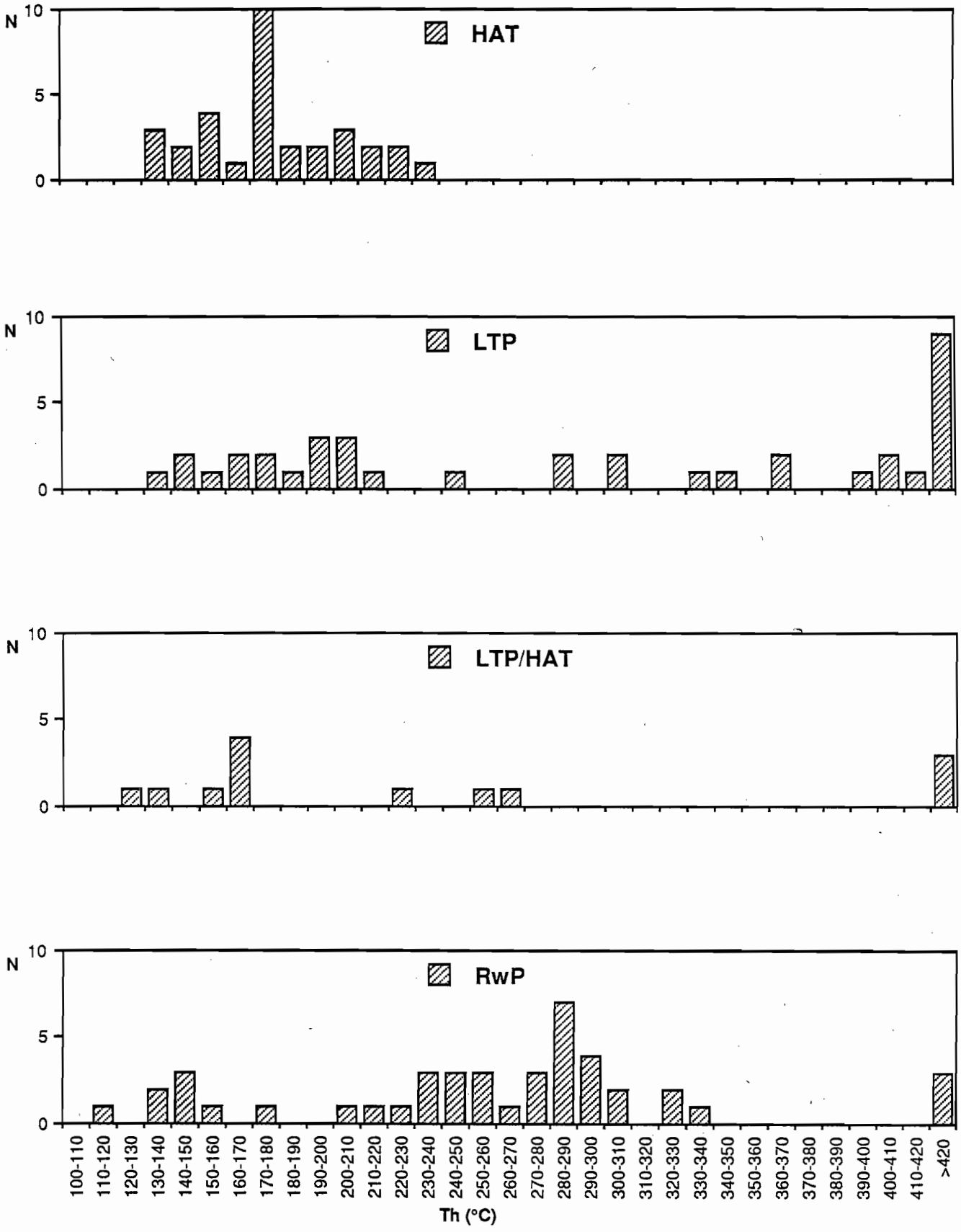

Figure 7. Homogenization temperatures of Type 2 fluid inclusions in various lithologies of the mine classification scheme. HAT="intensely altered volcaniclastic rock", LTP="lapilli tuff", LTP/HAT=combination of these, RwP="reworked pyroclastics".

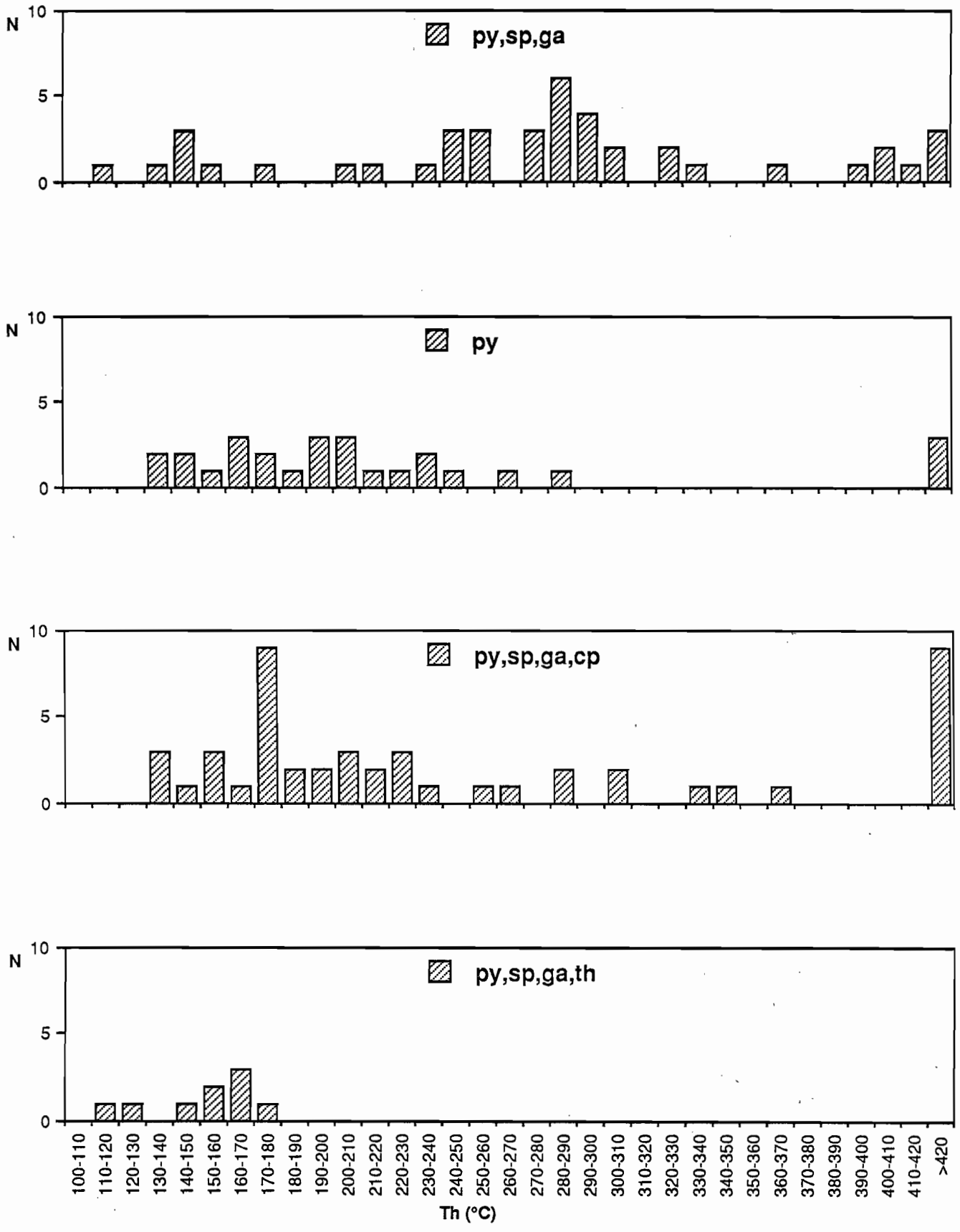

Figure 8. Homogenization temperatures of Type 2 fluid inclusions with main sulphide associations. py=pyrite, sp=sphalerite, ga=galena, cp=chalcopyrite, th=tetrahedrite.

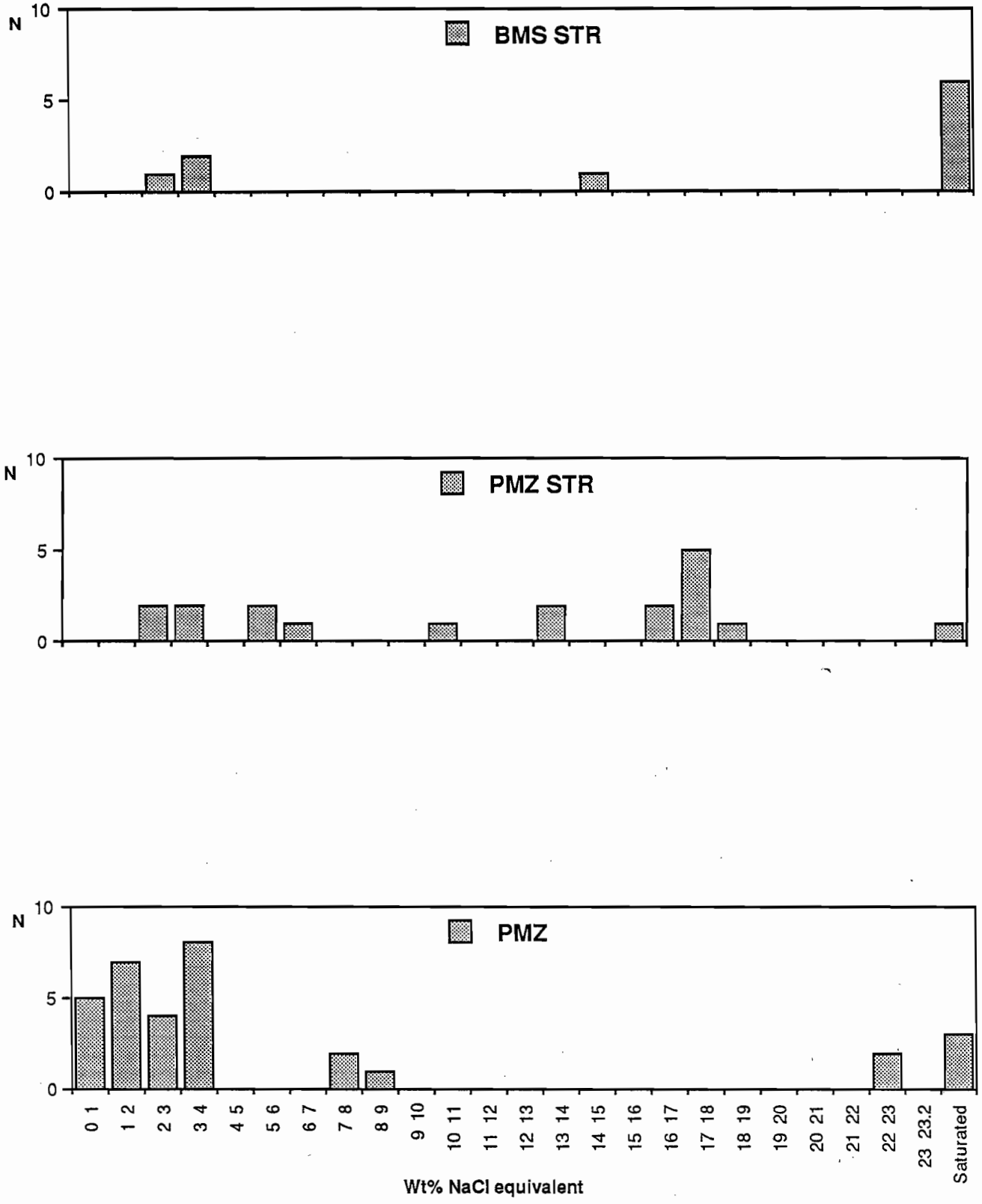

Figure 9. Weight% NaCl equivalent of Type 2 fluid inclusion contents in various parts of the system. BMS STR=stringers below sulphide orebodies, PMZ STR=stringers in lower part of precious metal zone, PMZ=precious metal zone.

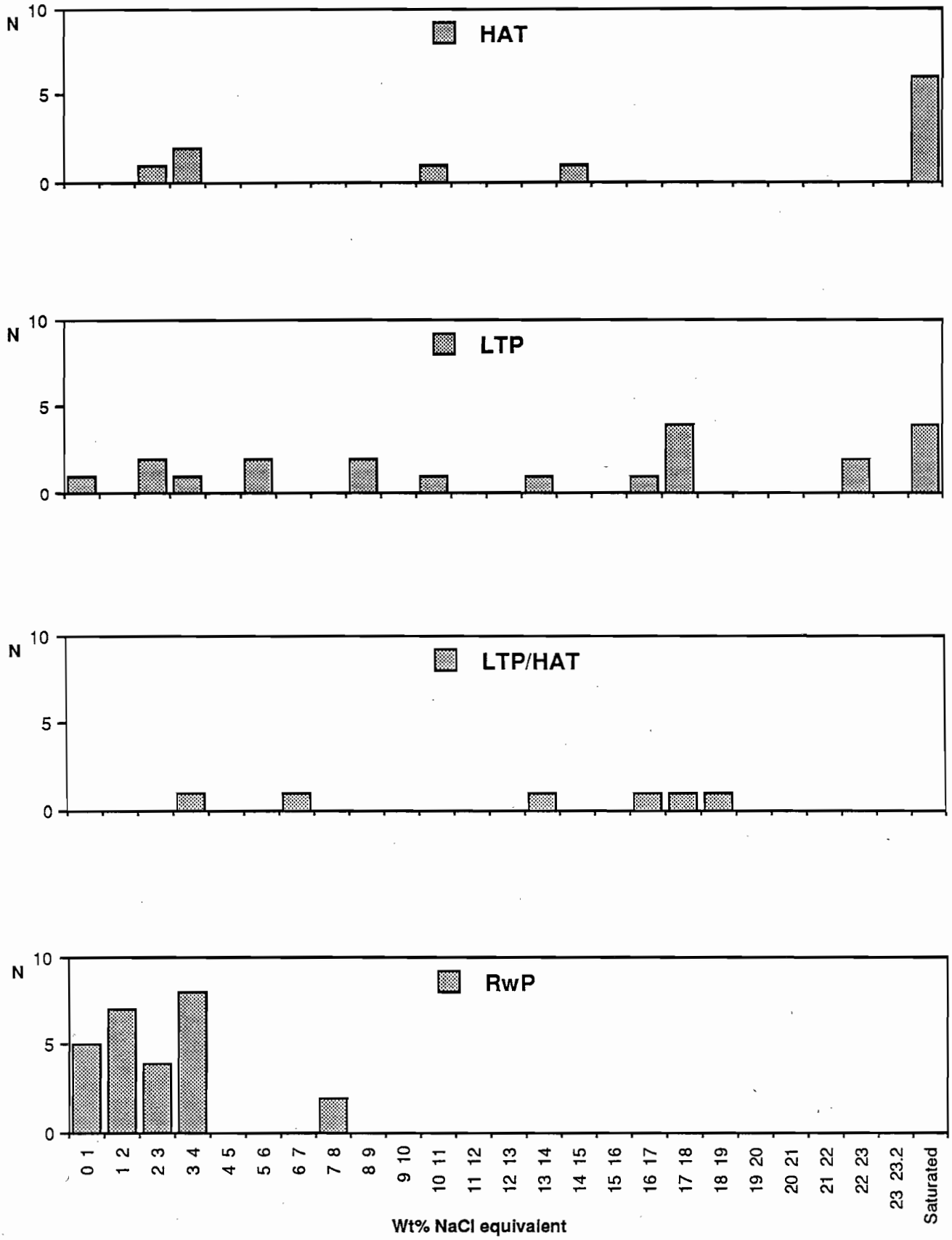

Figure 10. Weight% NaCl equivalent of Type 2 fluid inclusion contents in various lithologies of the mine classification scheme. HAT="intensely altered volcaniclastic rock", LTP="lapilli tuff", LTP/HAT=combination of these, RwP="reworked pyroclastics".

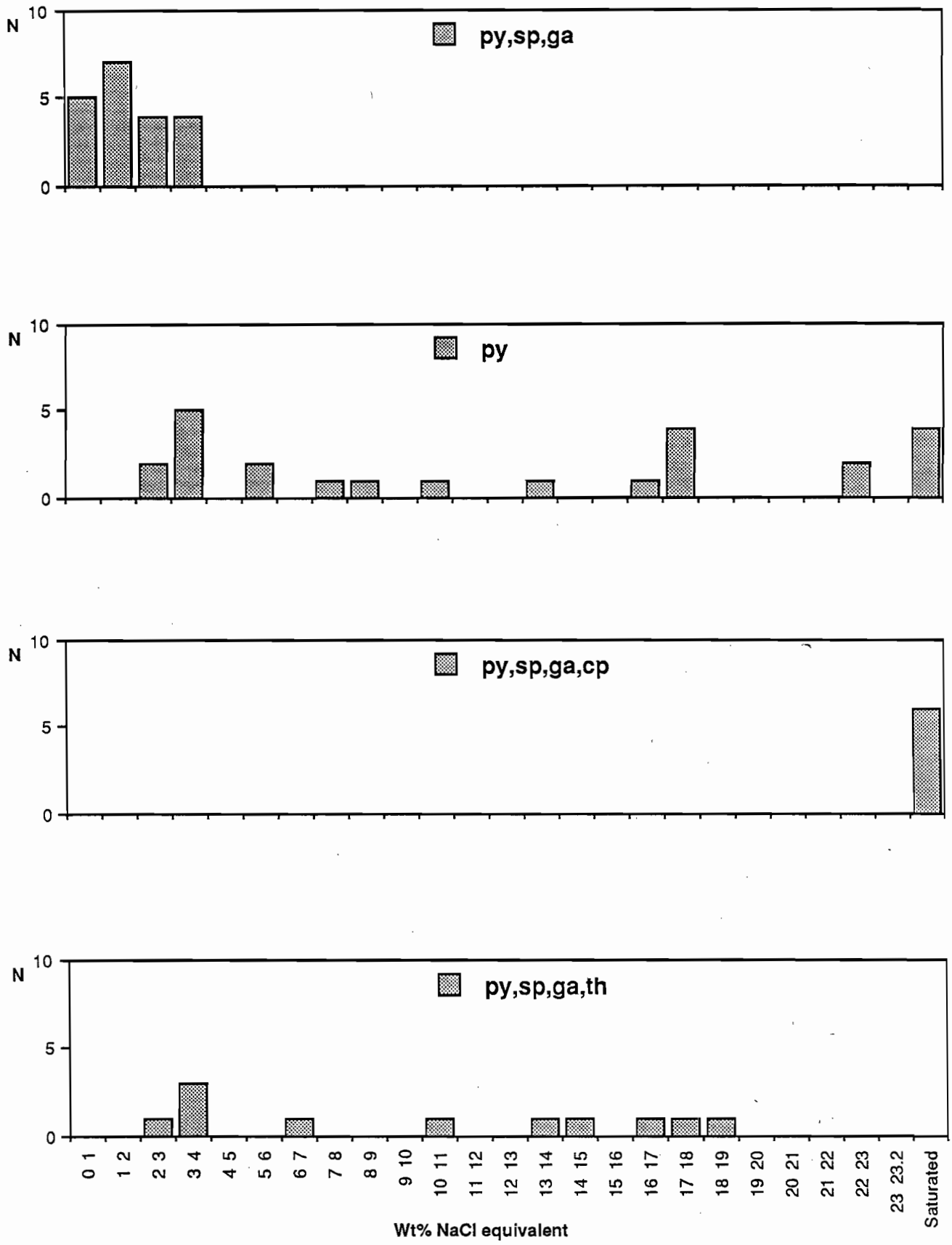

Figure 11. Weight% NaCl equivalent of Type 2 fluid inclusion contents with main sulphide associations. py=pyrite, sp=sphalerite, ga=galena, cp=chalcopyrite, th=tetrahedrite.

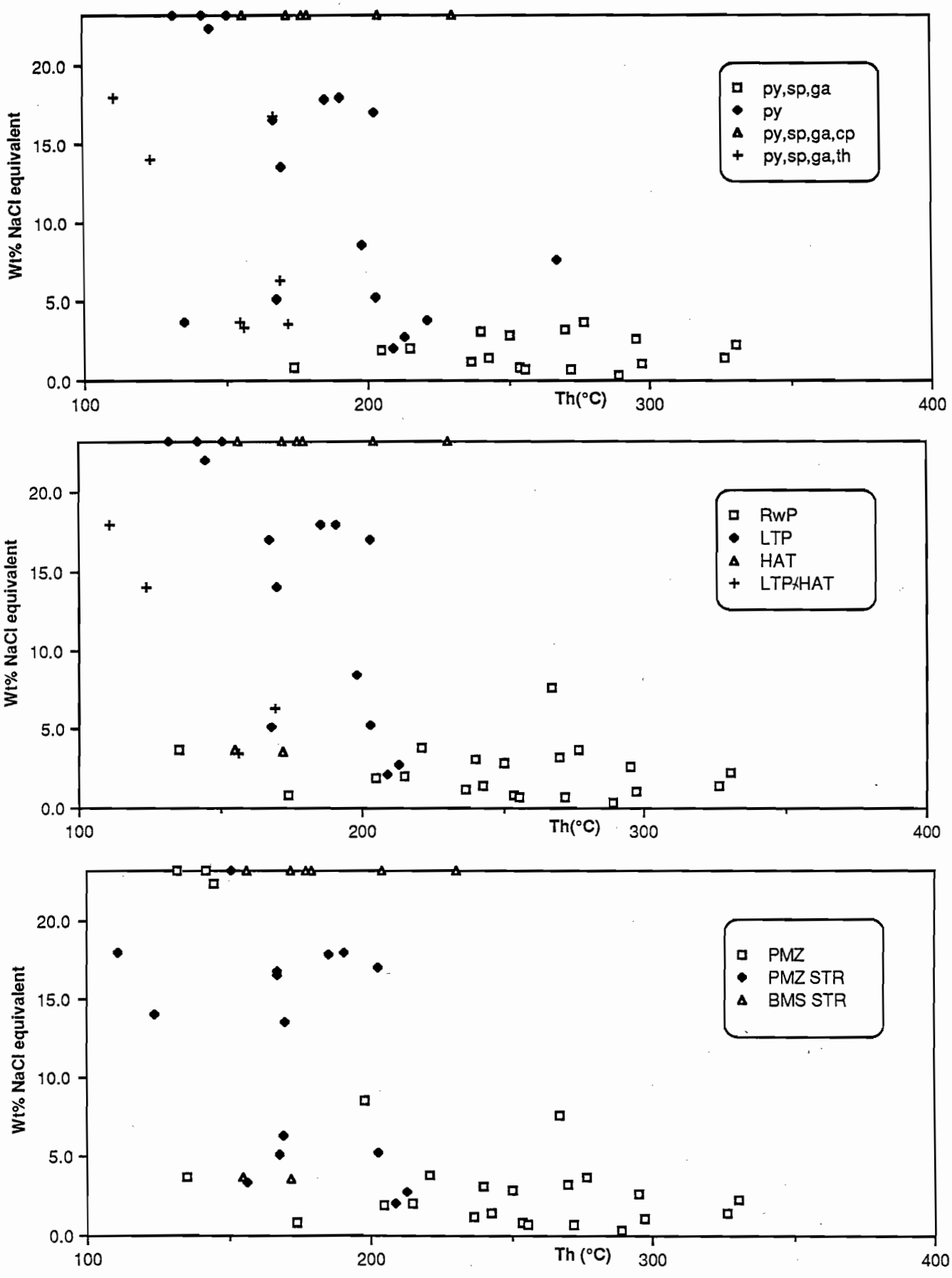

Figure 12. Plots of salinity against fluid inclusion homogenization temperature for different sulphide assemblages, lithologies and areas of the system. See previous figures for abbreviations.

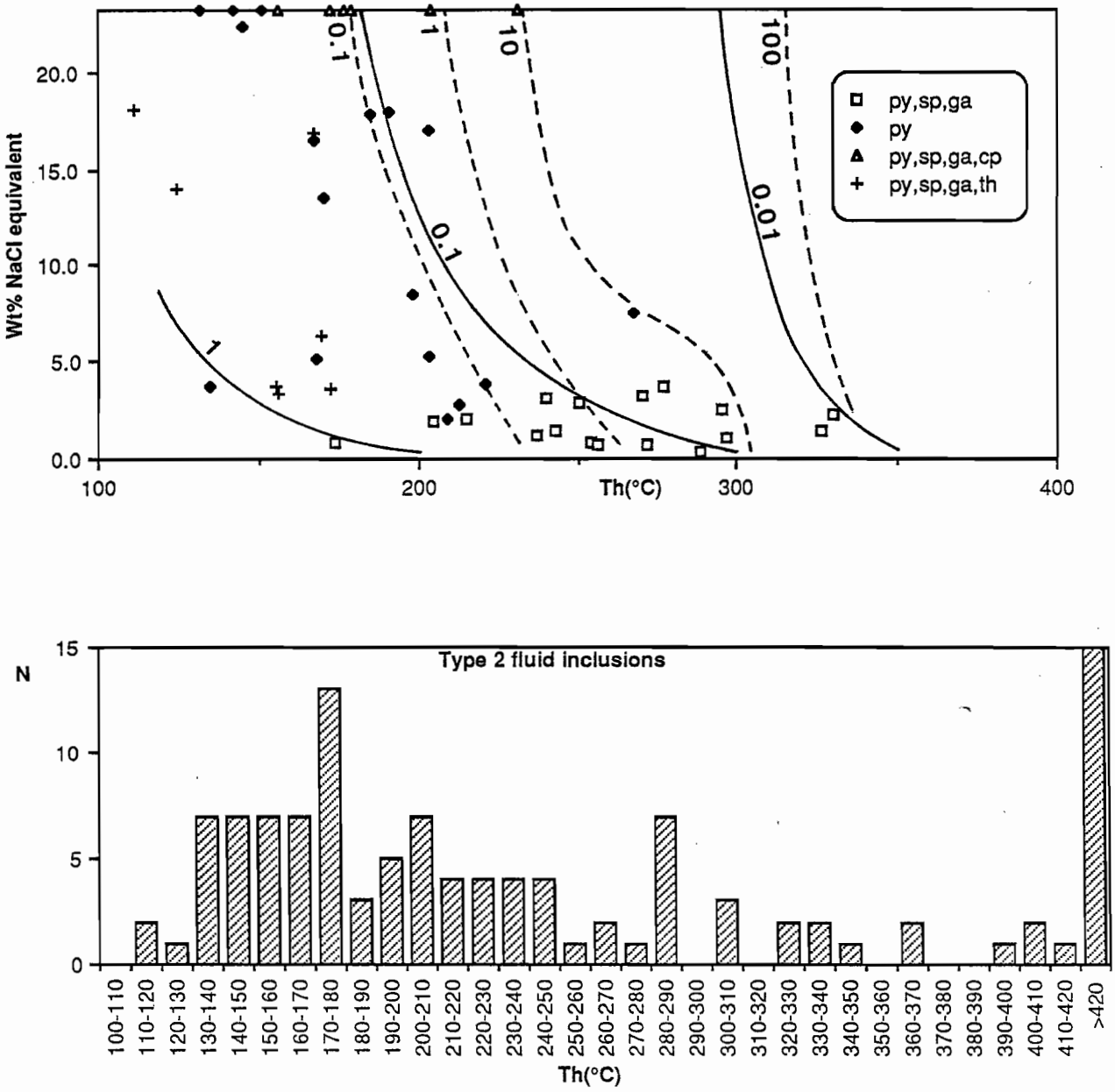

Figure 13. Solubility contours, in parts per million, for zinc as chloride complexes (dashed lines) and gold as bisulphide complexes (solid lines) superimposed on observed salinity and temperature data for different sulphide associations. Solubilities were calculated for pH=5.0, ΣS=0.003M, log $[SO_4]/[H_2S]$=-1.0. The histogram below shows homogenization temperatures for all Type 2 fluid inclusions including those for which salinities were not measurable.

APPENDIX

RAW THERMOMETRIC DATA

Measurements were made on a Fluid Inc® adapted U.S.G.S. type heating-freezing stage. Each result was produced by bracketing the temperature at which the relevant phase change occurred to within 1°C for homogenization measurements and 0.1°C for low temperature measurements. Calibration was by a set of Syn Flinc® synthetic fluid inclusion standards. The raw results are presented in the following table.

SAMPLE NUMBER	HOST MINERAL	FLUID INCLUSION TYPE	SIZE (μm)	LIQUID/ VAPOUR RATIO	TEMPERATURE OF FINAL MELTING OF ICE (°C)	TEMPERATURE OF HOMOGENIZ-ATION (°C)	HOMOGENIZ-ATION TO LIQUID (L) OR VAPOUR (V)	SALINITY (weight% NaCl equivalent)	HOST LITHOLOGY	HOST AREA	SULPHIDE AND TRANSPARENT MINERAL ASSOCIATION
				D=daughter							
				mineral				accurate to			py=pyrite
	BA=barite							1 decimal			sp=sphalerite
	QZ=quartz							place only;			ga=galena
	SP=sphalerite							extra digits			cp=chalcopyrite
		4=CO2						are result of			th=tetrahedrite
		2=primary						calculation			ba=barite
		1=secondary						program			qz=quartz
											ca=carbonate
											ru=rutile
											cpd=chalcopyrite disease
											in sphalerite
503001B	BA	2	9	80/20	-0.5	254	L	0.87426	RwP	PMZ	py,sp,ga,ba,qz
503001B	BA	2	15	80/20	-0.7			1.2181189	RwP	PMZ	py,sp,ga,ba,qz
503001B	BA	2	10	80/20		291	L		RwP	PMZ	py,sp,ga,ba,qz
503001B	BA	2	20	80/20	-0.8			1.3888085	RwP	PMZ	py,sp,ga,ba,qz
503001B	BA	2	9	80/20	-0.4	272	L	0.7010843	RwP	PMZ	py,sp,ga,ba,qz
503001B	BA	2	9	80/20	-0.4	256	L	0.7010843	RwP	PMZ	py,sp,ga,ba,qz
503001B	BA	2	20	70/30	-2			3.3738462	RwP	PMZ	py,sp,ga,ba,qz
503001B	BA	2	8	80/20	-0.2	289	L	0.3522249	RwP	PMZ	py,sp,ga,ba,qz
503001B	BA	2	10	80/20	-0.6	297	L	1.0466038	RwP	PMZ	py,sp,ga,ba,qz
503001B	BA	2	10	80/20		299	L		RwP	PMZ	py,sp,ga,ba,qz
503001B	BA	2	20	80/20		301	L		RwP	PMZ	py,sp,ga,ba,qz
503001B	BA	2	12	70/30		281	L		RwP	PMZ	py,sp,ga,ba,qz
503001B	BA	2	30	70/30	-2.2	277	L	3.6935572	RwP	PMZ	py,sp,ga,ba,qz
503001B	BA	2	12	70/30	-1.7	250	L	2.8883892	RwP	PMZ	py,sp,ga,ba,qz
503001B	BA	2	20	70/30	-1.5	295	L	2.5607873	RwP	PMZ	py,sp,ga,ba,qz
503001B	BA	2	10	70/30		247	L		RwP	PMZ	py,sp,ga,ba,qz
503001B	BA	2	12	70/30	-1.8	240	L	3.0509979	RwP	PMZ	py,sp,ga,ba,qz
503001B	BA	2	15	70/30	-1.9	270	L	3.2128158	RwP	PMZ	py,sp,ga,ba,qz
503001B	BA	2	12	70/30	-0.7	237	L	1.2181189	RwP	PMZ	py,sp,ga,ba,qz
503001B	BA	2	10	70/30	-0.8	243	L	1.3888085	RwP	PMZ	py,sp,ga,ba,qz
503001B	BA	2	8	85/15	-1.1	205	L	1.8959558	RwP	PMZ	py,sp,ga,ba,qz
503001B	BA	2	6	70/30	-1.3	330	L	2.2299846	RwP	PMZ	py,sp,ga,ba,qz
503001B	BA	2	10	80/20	-1.2	215	L	2.063375	RwP	PMZ	py,sp,ga,ba,qz
503001B	BA	2	20	80/20	-0.5	174	L	0.87426	RwP	PMZ	py,sp,ga,ba,qz
503001B	BA	2	10	20/80		>350	L		RwP	PMZ	py,sp,ga,ba,qz

503001B	BA	2	12	20/80		>350	L		RwP	PMZ	py,sp,ga,ba,qz
503001B	BA	2	10	70/30	-0.8	326	L	1.3888085	RwP	PMZ	py,sp,ga,ba,qz
503004	QZ	2	4	40/60		288	L		RwP	PMZ	py,sp,ga,qz
503004	QZ	2	3	90/10		286	L		RwP	PMZ	py,sp,ga,qz
503004	QZ	2	5	50/50		285	L		RwP	PMZ	py,sp,ga,qz
503004	QZ	2	5	50/50		285	L		RwP	PMZ	py,sp,ga,qz
503004	QZ	2	5	60/40		325	L		RwP	PMZ	py,sp,ga,qz
503004	QZ	1	5	80/20		140	L		RwP	PMZ	py,sp,ga,qz
503004	QZ	2	3	50/50		306	L		RwP	PMZ	py,sp,ga,qz
503004	QZ	1	5	90/10		165	L		RwP	PMZ	py,sp,ga,qz
503004	QZ	2	30	70/30	-4.5			7.152928	RwP	PMZ	py,sp,ga,qz
503004	QZ	2	5	70/30		>380	L		RwP	PMZ	py,sp,ga,qz
503007	QZ	2	6	80/20		113	L		RwP	PMZ	py,sp,ga,qz
503007	QZ	2	7	90/10		145	L		RwP	PMZ	py,sp,ga,qz
503007	QZ	1	4	90/10		180	L		RwP	PMZ	py,sp,ga,qz
503007	QZ	2	6	90/10		145	L		RwP	PMZ	py,sp,ga,qz
503007	QZ	2	5	80/20		146	L		RwP	PMZ	py,sp,ga,qz
503007	QZ	2	6	80/20		150	L		RwP	PMZ	py,sp,ga,qz
503007	QZ	2	3	80/20		131	L		RwP	PMZ	py,sp,ga,qz
503008	QZ	1	10	80/20	-9.4	151	L	13.327367	RwP	PMZ	py,ga,(sp),qz,ca
503008	QZ	1	12	80/20	-9.5	168	L	13.438359	RwP	PMZ	py,ga,(sp),qz,ca
503008	QZ	1	18	80/20	-9.3	178	L	13.215825	RwP	PMZ	py,ga,(sp),qz,ca
503008	QZ	1	20	80/20	-9.8	186	L	13.768067	RwP	PMZ	py,ga,(sp),qz,ca
503008	QZ	1	18	80/20					RwP	PMZ	py,ga,(sp),qz,ca
503008	QZ	1	30	80/20	-10.7	133	L	14.728515	RwP	PMZ	py,ga,(sp),qz,ca
503008	QZ	1	20	80/20	-10.4			14.413059	RwP	PMZ	py,ga,(sp),qz,ca
503008	QZ	1	20	80/20	-10.5	153	L	14.518725	RwP	PMZ	py,ga,(sp),qz,ca
503008	QZ	1	30	80/20	-10.9	139	L	14.936269	RwP	PMZ	py,ga,(sp),qz,ca
503008	QZ	1	15	80/20	-11.2	138	L	15.24414	RwP	PMZ	py,ga,(sp),qz,ca
503008	QZ	1	60	80/20		141	L		RwP	PMZ	py,ga,(sp),qz,ca
503008	QZ	1	15	80/20	-10.3	183	L	14.306875	RwP	PMZ	py,ga,(sp),qz,ca
503008	QZ	1	15	80/20	-9.1	181	L	12.991079	RwP	PMZ	py,ga,(sp),qz,ca
503008	QZ	1	15	80/20	-10.1	172	L	14.092938	RwP	PMZ	py,ga,(sp),qz,ca
503008	QZ	1	30	80/20	-2.6	170	L	4.3236684	RwP	PMZ	py,ga,(sp),qz,ca
503008	QZ	1	20	80/20	-0.1	157	L	0.1765347	RwP	PMZ	py,ga,(sp),qz,ca
503008	QZ	1	15	80/20	-0.3	186	L	0.5270737	RwP	PMZ	py,ga,(sp),qz,ca
503008	QZ	1	25	80/20	-0.1	153	L	0.1765347	RwP	PMZ	py,ga,(sp),qz,ca
503008	QZ	1	25	80/20	-10.3	151	L	14.306875	RwP	PMZ	py,ga,(sp),qz,ca
503008	QZ	1	5	80/20	-10.5	145	L	14.518725	RwP	PMZ	py,ga,(sp),qz,ca
503008	QZ	1	30	80/20	-9.8	142	L	13.768067	RwP	PMZ	py,ga,(sp),qz,ca
503008	QZ	1	20	80/20	-8.9	121	L	12.764094	RwP	PMZ	py,ga,(sp),qz,ca

503008	QZ	1	20	80/20	-9.9	153	L	13.876891	RwP	PMZ	py,ga,(sp),qz,ca
503008	QZ	1	10	80/20	-9.7	120	L	13.658706	RwP	PMZ	py,ga,(sp),qz,ca
503008	QZ	1	20	80/20	-11.4	165	L	15.446917	RwP	PMZ	py,ga,(sp),qz,ca
503008	QZ	1	8	80/20	-12.4	187	L	16.432106	RwP	PMZ	py,ga,(sp),qz,ca
503008	QZ	1	20	80/20	-12.5	182	L	16.52807	RwP	PMZ	py,ga,(sp),qz,ca
503008	QZ	1	15	80/20	-12.8	184	L	16.813264	RwP	PMZ	py,ga,(sp),qz,ca
503008	QZ	1	10	80/20	-12.2	197	L	16.23881	RwP	PMZ	py,ga,(sp),qz,ca
503008	QZ	1	20	80/20	-11	152	L	15.039391	RwP	PMZ	py,ga,(sp),qz,ca
503008	QZ	1	30	80/20	-11	163	L	15.039391	RwP	PMZ	py,ga,(sp),qz,ca
502689	BA	1	15	90/10	-0.6	155	L	1.0466038	LTP	PMZ	py,sp,(ga),(cp),ba,qz
502689	BA	1	15	90/10		157	L		LTP	PMZ	py,sp,(ga),(cp),ba,qz
502689	BA	1	5	80/20		191	L		LTP	PMZ	py,sp,(ga),(cp),ba,qz
502689	BA	1	8	80/20		180	L		LTP	PMZ	py,sp,(ga),(cp),ba,qz
502689	BA	1	8	80/20	-0.5	178	L	0.87426	LTP	PMZ	py,sp,(ga),(cp),ba,qz
502689	BA	2	10	30/70		>420	L		LTP	PMZ	py,sp,(ga),(cp),ba,qz
502689	BA	2	8	30/70		>420	L		LTP	PMZ	py,sp,(ga),(cp),ba,qz
502689	BA	2	10	20/80		361	L		LTP	PMZ	py,sp,(ga),(cp),ba,qz
502689	BA	2	10	70/30		>420	L		LTP	PMZ	py,sp,(ga),(cp),ba,qz
502689	BA	1	6	80/20	-0.3	237	L	0.5270737	LTP	PMZ	py,sp,(ga),(cp),ba,qz
502689	BA	1	6	80/20	-0.1	220	L	0.1765347	LTP	PMZ	py,sp,(ga),(cp),ba,qz
502689	BA	1	15	80/20	-0.1	147	L	0.1765347	LTP	PMZ	py,sp,(ga),(cp),ba,qz
502689	BA	1	10	80/20	-0.2	176	L	0.3522249	LTP	PMZ	py,sp,(ga),(cp),ba,qz
502689	BA	1	12	80/20	-0.1	181	L	0.1765347	LTP	PMZ	py,sp,(ga),(cp),ba,qz
502689	QZ	2	4	50/50		308	L		LTP	PMZ	py,sp,(ga),(cp),ba,qz
502689	QZ	2	6	50/50		282	L		LTP	PMZ	py,sp,(ga),(cp),ba,qz
502689	QZ	2	10	40/60		286	L		LTP	PMZ	py,sp,(ga),(cp),ba,qz
502689	QZ	2	5	40/60		343	L		LTP	PMZ	py,sp,(ga),(cp),ba,qz
502689	QZ	2	6	40/60		336	L		LTP	PMZ	py,sp,(ga),(cp),ba,qz
502689	QZ	2	8	50/50		305	L		LTP	PMZ	py,sp,(ga),(cp),ba,qz
502689	QZ	2	4	30/70		>500	L		LTP	PMZ	py,sp,(ga),(cp),ba,qz
502689	QZ	2	4	30/70		>500	L		LTP	PMZ	py,sp,(ga),(cp),ba,qz
502689	QZ	2	4	30/70		>500	L		LTP	PMZ	py,sp,(ga),(cp),ba,qz
502897	BA	1	6	90/10	-2	148	L	3.3738462		PMZ	
502897	BA	1	12	90/10	-2.7	141	L	4.4792749		PMZ	
502897	BA	1	15	90/10	-2.1	142	L	3.5340923		PMZ	
503011	BA	2	25	80/20	-2.3	221	L	3.8522441	RwP	PMZ	py,ba,ru
503011	BA	2	10	80/20	-2.2	135	L	3.6935572	RwP	PMZ	py,ba,ru
503011	BA	2	15	80/20	-2			3.3738462	RwP	PMZ	py,ba,ru
503011	BA	2	8	80/20		233	L		RwP	PMZ	py,ba,ru
503011	BA	2	8	80/20		237	L		RwP	PMZ	py,ba,ru
503011	BA	2	5	80/20		280	L		RwP	PMZ	py,ba,ru

503011	BA	2	10	80/20	-2.1			3.5340923	RwP	PMZ	py,ba,ru
503011	BA	2	5	80/20	-4.8	267	L	7.5758249	RwP	PMZ	py,ba,ru
503011	BA	1	12	80/20	-0.8	153	L	1.3888085	RwP	PMZ	py,ba,ru
503011	BA	1	10	80/20	-0.8	161	L	1.3888085	RwP	PMZ	py,ba,ru
503011	BA	1	8	80/20	-0.7	155	L	1.2181189	RwP	PMZ	py,ba,ru
503096	QZ	2	12	80/20	-19.4			22.231734	LTP	PMZ	py,(ga),(sp),qz,ca
503096	QZ	2	8	80/20	-5.5	198	L	8.5383834	LTP	PMZ	py,(ga),(sp),qz,ca
503096	QZ	2	12	80/20+D	-22.3	132	L	24.237346	LTP	PMZ	py,(ga),(sp),qz,ca
503096	QZ	2	10	80/20	-19.6	145	L	22.375469	LTP	PMZ	py,(ga),(sp),qz,ca
503096	QZ	2	5	80/20	-24.6	142	L	25.739594	LTP	PMZ	py,(ga),(sp),qz,ca
503096	QZ	2	15	80/20	-22			24.036705	LTP	PMZ	py,(ga),(sp),qz,ca
503145	QZ	2	5	80/20	-3.2	203	L	5.2459381	LTP	PMZ STR	py,ba,qz
503145	QZ	2	5	80/20	-2.2			3.6935572	LTP	PMZ STR	py,ba,qz
503145	QZ	2	5	80/20		241	L		LTP	PMZ STR	py,ba,qz
503145	QZ	2	10	80/20		177	L		LTP	PMZ STR	py,ba,qz
503145	QZ	2	5	80/20	-1.6	213	L	2.7249867	LTP	PMZ STR	py,ba,qz
503145	QZ	2	10	80/20	-1.2	209	L	2.063375	LTP	PMZ STR	py,ba,qz
503145	QZ	2	12	80/20	-3.1	168	L	5.0941109	LTP	PMZ STR	py,ba,qz
503145	QZ	2	6	80/20	-25.1	151	L	26.060032	LTP	PMZ STR	py,ba,qz
503145	QZ	2	12	80/20+D	-13	203	L	17.001177	LTP	PMZ STR	py,ba,qz
503145	QZ	2	10	80/20+D	-14	191	L	17.915084	LTP	PMZ STR	py,ba,qz
503145	QZ	2	40	80/20+D	-13.9	185	L	17.825565	LTP	PMZ STR	py,ba,qz
503145	QZ	2	10	80/20	-13.2			17.187345	LTP	PMZ STR	py,ba,qz
503145	QZ	2	8	80/20	-7.1			10.616339	LTP	PMZ STR	py,ba,qz
503145	QZ	2	12	80/20	-1.2?	197	L		LTP	PMZ STR	py,ba,qz
503145	QZ	2	20	80/20	-12.5	167	L	16.52807	LTP	PMZ STR	py,ba,qz
503145	QZ	2	12	80/20	-9.6	170	L	13.548805	LTP	PMZ STR	py,ba,qz
503148A	QZ	1	5	80/20		208	L		HAT	BMS STR	py,sp,ga,cp,qz,ba,ca
503148A	QZ	1	20	80/20			L		HAT	BMS STR	py,sp,ga,cp,qz,ba,ca
503148A	QZ	2	3	60/40		228	L		HAT	BMS STR	py,sp,ga,cp,qz,ba,ca
503148A	BA	1	4	80/20		186	L		HAT	BMS STR	py,sp,ga,cp,qz,ba,ca
503148A	BA	1	8	80/20		196	L		HAT	BMS STR	py,sp,ga,cp,qz,ba,ca
503148A	QZ	2	6			207	L		HAT	BMS STR	py,sp,ga,cp,qz,ba,ca
503148A	QZ	2	4			178	L		HAT	BMS STR	py,sp,ga,cp,qz,ba,ca
503148B	QZ	4	15	20/CO240/40					HAT	BMS STR	py,sp,ga,cp,qz,ba,ca
503148B	QZ	4	5	20/CO240/40		310	V		HAT	BMS STR	py,sp,ga,cp,qz,ba,ca
503148B	QZ	2	10	80/20+D	-23.5	204	L	25.028029	HAT	BMS STR	py,sp,ga,cp,qz,ba,ca
503148B	QZ	4	5	20/CO240/40		285	V		HAT	BMS STR	py,sp,ga,cp,qz,ba,ca
503148B	QZ	2	8	80/20	-23	231	L	24.700703	HAT	BMS STR	py,sp,ga,cp,qz,ba,ca
503148B	QZ	2	8	80/20+D	-23.7	179	L	25.158212	HAT	BMS STR	py,sp,ga,cp,qz,ba,ca
503148B	QZ	2	6	80/20+D	-23.3	177	L	24.897431	HAT	BMS STR	py,sp,ga,cp,qz,ba,ca

503148B	QZ	2	12	80/20+D	-23.2	172	L	24.831969	HAT	BMS STR	py,sp,ga,cp,qz,ba,ca
503148B	QZ	2	8	80/20+D	-22.9	156	L	24.634893	HAT	BMS STR	py,sp,ga,cp,qz,ba,ca
503151A	QZ	1	3	90/10		137	L		LTP/HAT	PMZ-DBS	py,sp,ga,cp,qz
503151A	QZ	1	3			174	L		LTP/HAT	PMZ-DBS	py,sp,ga,cp,qz
503151A	QZ	1	3			155	L		LTP/HAT	PMZ-DBS	py,sp,ga,cp,qz
503151A	QZ	1	3			150	L		LTP/HAT	PMZ-DBS	py,sp,ga,cp,qz
503151A	QZ	1	3			145	L		LTP/HAT	PMZ-DBS	py,sp,ga,cp,qz
503100	QZ	2	8	50/10D40					HAT/LTP	PMZ-DBS	py,qz
503100	QZ	2	8	550/10D40		138	L		HAT/LTP	PMZ-DBS	py,qz
503100	QZ	2	8	50/10D40					HAT/LTP	PMZ-DBS	py,qz
503100	QZ	2	5	50/10D40		165	L		HAT/LTP	PMZ-DBS	py,qz
503100	QZ	2	12	40/10D50					HAT/LTP	PMZ-DBS	py,qz
503033	QZ	1	10	80/20	-1.8	139	L	3.0509979	HAT/LTP	PMZ	py,sp,ga,(cp),qz,ba
503033	QZ	1	30	80/20	0	153	L	0	HAT/LTP	PMZ	py,sp,ga,(cp),qz,ba
503033	QZ	1	15	80/20					HAT/LTP	PMZ	py,sp,ga,(cp),qz,ba
503033	QZ	1	7	80/20	0	148	L	0	HAT/LTP	PMZ	py,sp,ga,(cp),qz,ba
503033	QZ	1	10	90/10	-0.2	150	L	0.3522249	HAT/LTP	PMZ	py,sp,ga,(cp),qz,ba
503033	QZ	1	10	90/10	-11.3	155	L	15.345773	HAT/LTP	PMZ	py,sp,ga,(cp),qz,ba
503033	QZ	1	15	90/10	-10.4	150	L	14.413059	HAT/LTP	PMZ	py,sp,ga,(cp),qz,ba
503033	QZ	1	20	90/10	-0.7	125	L	1.2181189	HAT/LTP	PMZ	py,sp,ga,(cp),qz,ba
503033	QZ	1	15	90/10	-0.6	199	L	1.0466038	HAT/LTP	PMZ	py,sp,ga,(cp),qz,ba
503109B	QZ	2	20	80/20	-14.1	111	L	18.004199	HAT/LTP	PMZ STR	py,sp,ga,th,qz
503109B	QZ	2	8	80/20		163	L		HAT/LTP	PMZ STR	py,sp,ga,th,qz
503109B	QZ	2	10	80/20	-13			17.001177	HAT/LTP	PMZ STR	py,sp,ga,th,qz
503109B	QZ	2	12	80/20	-3.9	169	L	6.2880087	HAT/LTP	PMZ STR	py,sp,ga,th,qz
503109B	QZ	2	15	80/20	-12.8	167	L	16.813264	HAT/LTP	PMZ STR	py,sp,ga,th,qz
503109B	QZ	2	12	80/20	-2	156	L	3.3738462	HAT/LTP	PMZ STR	py,sp,ga,th,qz
503109B	QZ	2	10	80/20+D	-10	124	L	13.98518	HAT/LTP	PMZ STR	py,sp,ga,th,qz
503121	QZ	2	7	90/10	-7.2			10.740782	HAT	BMS STR	py,sp,ga,th,cpd,qz
503121	QZ	2	12	80/20	-1.3			2.2299846	HAT	BMS STR	py,sp,ga,th,cpd,qz
503121	QZ	2	3	60/40	-5.9?				HAT	BMS STR	py,sp,ga,th,cpd,qz
503121	QZ	2	12	80/20	-10.2			14.200169	HAT	BMS STR	py,sp,ga,th,cpd,qz
503121	QZ	2	15	80/20	-2.2	155	L	3.6935572	HAT	BMS STR	py,sp,ga,th,cpd,qz
503121	QZ	2	20	90/10	-2.1	172	L	3.5340923	HAT	BMS STR	py,sp,ga,th,cpd,qz
503121	QZ	2	3	60/40	-5.5?				HAT	BMS STR	py,sp,ga,th,cpd,qz
503121	QZ	2	10	80/20		148	L		HAT	BMS STR	py,sp,ga,th,cpd,qz
503121	QZ	1	12	80/20		165	L		HAT	BMS STR	py,sp,ga,th,cpd,qz
503121	QZ	4	12	20CO240/40					HAT	BMS STR	py,sp,ga,th,cpd,qz
503121	QZ	4	15	20CO240/40					HAT	BMS STR	py,sp,ga,th,cpd,qz
503121	QZ	1	10	80/20		178	L		HAT	BMS STR	py,sp,ga,th,cpd,qz
503121	QZ	1	8	80/20		140	L		HAT	BMS STR	py,sp,ga,th,cpd,qz

503011	QZ	2	3	60/40		>420	L		RwP	PMZ	py,ba,ru
503011	QZ	2	3	60/40		>420	L		RwP	PMZ	py,ba,ru
503011	QZ	2	3	60/40		>420	L		RwP	PMZ	py,ba,ru
503109A	QZ	1	15	60/40	-8.1	177	L	11.833268	HAT/LTP	PMZ STR	py,(ga),(sp),qz
503109A	QZ	1	12	70/30		130	L		HAT/LTP	PMZ STR	py,(ga),(sp),qz
503114	QZ	2	5	60/40		227	L		HAT/LTP	PMZ STR	py,(sp),(cp),qz,carb,ru
503114	QZ	2	3	60/40		266	L		HAT/LTP	PMZ STR	py,(sp),(cp),qz,carb,ru
503114	QZ	2	3	60/40		254	L		HAT/LTP	PMZ STR	py,(sp),(cp),qz,carb,ru
503114	QZ	2	3	80/20		>420	L		HAT/LTP	PMZ STR	py,(sp),(cp),qz,carb,ru
503114	QZ	2	3	80/20		>420	L		HAT/LTP	PMZ STR	py,(sp),(cp),qz,carb,ru
503114	QZ	2	3	80/20		>420	L		HAT/LTP	PMZ STR	py,(sp),(cp),qz,carb,ru
503118	QZ	2	10	60/40		364	L		LTP	BMS	py,sp,ga,qz
503118	QZ	2	3	80/20		405	L		LTP	BMS	py,sp,ga,qz
503118	QZ	2	3	60/40		>460	L		LTP	BMS	py,sp,ga,qz
503118	QZ	2	3	60/40		>460	L		LTP	BMS	py,sp,ga,qz
503118	QZ	2	3	60/40		>460	L		LTP	BMS	py,sp,ga,qz
503118	SP	1	10	80/20	-6.3	186	L	9.5981028	LTP	BMS	py,sp,ga,qz
503118	SP	1	5	80/20+D	-5.8	194	L	8.9407425	LTP	BMS	py,sp,ga,qz
503118	SP	1	15	80/20	-6.5			9.8564876	LTP	BMS	py,sp,ga,qz
503118	QZ	2	3	70/30		406	V		LTP	BMS	py,sp,ga,qz
503118	QZ	2	6	60/40		398	V		LTP	BMS	py,sp,ga,qz
503118	QZ	2	3	60/40		415	V		LTP	BMS	py,sp,ga,qz
503045	QZ	2	4	60/40		>340	L				
503132	QZ	2	15	80/20		194	L		HAT	BMS STR	py,sp,ga,cpd,qz
503132	QZ	2	6	80/20		168	L		HAT	BMS STR	py,sp,ga,cpd,qz
503132	QZ	2	20	80/20		196	L		HAT	BMS STR	py,sp,ga,cpd,qz
503132	QZ	2	6	80/20		183	L		HAT	BMS STR	py,sp,ga,cpd,qz
503132	QZ	2	8	80/20		174	L		HAT	BMS STR	py,sp,ga,cpd,qz
503132	QZ	2	5	80/20		175	L		HAT	BMS STR	py,sp,ga,cpd,qz
503132	QZ	2	12	80/20		147	L		HAT	BMS STR	py,sp,ga,cpd,qz
503132	QZ	2	8	80/20		176	L		HAT	BMS STR	py,sp,ga,cpd,qz
503132	QZ	2	4	80/20		132	L		HAT	BMS STR	py,sp,ga,cpd,qz
503132	QZ	2	3	80/20		130	L		HAT	BMS STR	py,sp,ga,cpd,qz
503132	QZ	2	5	80/20		136	L		HAT	BMS STR	py,sp,ga,cpd,qz
503132	QZ	2	8	80/20		226	L		HAT	BMS STR	py,sp,ga,cpd,qz
503132	QZ	2	10	80/20		177	L		HAT	BMS STR	py,sp,ga,cpd,qz
503132	QZ	2	8	80/20		184	L		HAT	BMS STR	py,sp,ga,cpd,qz
503132	QZ	2	10	80/20		206	L		HAT	BMS STR	py,sp,ga,cpd,qz
503132	QZ	2	10	80/20		215	L		HAT	BMS STR	py,sp,ga,cpd,qz
503132	QZ	2	10	80/20		172	L		HAT	BMS STR	py,sp,ga,cpd,qz
503132	QZ	2	6	80/20		154	L		HAT	BMS STR	py,sp,ga,cpd,qz

503132	QZ	2	5	80/20		151	L		HAT	BMS STR	py,sp,ga,cpd,qz
503132	QZ	2	7	80/20		218	L		HAT	BMS STR	py,sp,ga,cpd,qz